

# Adaptive Control of Joystick Steering in Recreational Boats

John Bayless  
*Marquette University*

---

## Recommended Citation

Bayless, John, "Adaptive Control of Joystick Steering in Recreational Boats" (2017). *Master's Theses (2009 -)*. 437.  
[http://epublications.marquette.edu/theses\\_open/437](http://epublications.marquette.edu/theses_open/437)

ADAPTIVE CONTROL OF JOYSTICK STEERING IN RECREATIONAL BOATS

by

John A. Bayless, B.S., M.B.A.

A Thesis submitted to the Faculty of the Graduate School  
Marquette University  
in Partial Fulfillment of the Requirements for  
the Degree of Master of Science

Milwaukee, Wisconsin

August 2017

ABSTRACT  
ADAPTIVE CONTROL OF JOYSTICK STEERING IN RECREATIONAL BOATS

John A. Bayless, B.S., M.B.A.

Marquette University, 2017

This thesis addresses the challenge of commissioning recreational boats with joystick control when the boat's physical parameters are not known. The research was conducted by following a model-based, systems engineering approach which leveraged MATLAB simulations and scale-model physical testing. The outcome of the research is a working methodology using L1 Adaptive Control which provides fast adaption in a way that could reduce the cost of commissioning recreational boats with joystick control, improve the robustness of the final design, and potentially expand the accessible market to new boat types.

## ACKNOWLEDGEMENTS

John A. Bayless, B.S., M.B.A.

Thank you, Dr. Voglewede and Dr. Craig, for mentorship and support in pursuing this research. I would also like to thank Dr. Huang and Dr. Fleischmann for serving as committee members.

I am indebted to *Mercury Marine, a division of Brunswick Corporation* for sponsoring my graduate courses and to my former colleagues in Mercury's Product Development and Engineering department who inspired the research.

Finally, I owe the deepest gratitude to my dear family; Beth, Katie, and Brooke, for supporting me throughout the process. This thesis would neither be possible nor meaningful without your love.

## TABLE OF CONTENTS

ACKNOWLEDGEMENTS.....	i
LIST OF TABLES .....	iv
LIST OF FIGURES.....	vi
I. INTRODUCTION.....	1
A. Background .....	1
B. Statement of the Problem.....	3
C. Statement of the Procedure .....	8
II. PHYSICAL AND MATHEMATICAL MODELS.....	11
A. Introduction .....	11
B. Reference Frames .....	11
C. Rigid-Body Kinematics and Kinetics .....	12
III. CONTROL STRATEGY .....	21
A. Introduction .....	21
B. Adaptive Control Historical Perspective .....	21
C. Adaptive Joystick Control Problem Detail .....	24
D. L1 Adaptive Control.....	26
E. Designing the L1 Adaptive Control for the Test Boat.....	32
IV. SIMULATION RESULTS .....	41
V. TEST RESULTS.....	49
A. Test Equipment.....	49
B. Test Method.....	53
C. Test Cases.....	54
D. Test Procedure.....	57
E. Test Data .....	58

F. Test Results .....	68
G. Test Result Synthesis and Controller Refinements .....	70
VI. CONCLUSIONS AND OPPORTUNITIES FOR FURTHER RESEARCH.....	73
A. Conclusions .....	73
B. Contributions .....	74
C. Implications for Application .....	75
VII. BIBLIOGRAPHY AND REFERENCES.....	78
APPENDIX A Test Boat and Joystick Target Applications .....	81
APPENDIX C Materials.....	84
APPENDIX D MATLAB Projection Operator .....	85
APPENDIX E Test Plan and Test Procedure .....	86
APPENDIX F Yaw Maneuver Error Calculations .....	88
APPENDIX G Wiring Diagram.....	89
APPENDIX H Arduino Control Code for Sway Maneuvers .....	90

## LIST OF TABLES

Table 1 Performance Requirements .....	5
Table 2 Through and Across Variables in the Joystick Control System.....	7
Table 3 Model Based Systems Engineering Approach .....	9
Table 4 Coordinate System.....	12
Table 5 Factors in Controlling Recreation Boats with a Joystick.....	26
Table 6 L1 Adaptive Control Features .....	32
Table 7 Surge Subsystem Reference Model Step Input Response .....	33
Table 8 Sway/Yaw Subsystem Reference Model Step Input Response.....	34
Table 9 Actuator Physical and Mathematical Models.....	36
Table 10 Light Weight Narrow Motors Plant Parameters .....	42
Table 11 Light Weight Wide Motors Plant Parameters .....	43
Table 12 Light Weight Wide Motors Parameters .....	44
Table 13 Heavy Weight Narrow Motors Parameters .....	45
Table 14 Heavy Weight Wide Motors Parameters .....	46
Table 15 Test Boat and Target Application Froude Numbers .....	50
Table 16 Test Boat and Target Application Images.....	51
Table 17 Test Boat and Target Application Characteristics .....	52
Table 18 Sway Test Scenarios .....	55
Table 19 Yaw Test Scenarios .....	56
Table 20 Wind Disturbance Effects .....	57
Table 21 Commanded Inputs.....	58
Table 22 Sway Test Error Calculations .....	60
Table 23 Yaw Test Error Calculations .....	61
Table 24 Sway Test Data.....	62
Table 25 Yaw Test Data .....	66

Table 26 Sway Test Rank Order by Maximum Surge and Yaw Rate Error .....	72
Table 27 Physical System .....	83
Table 28 Materials List .....	84
Table 29 Test Procedure .....	87



## LIST OF FIGURES

Figure 1 Joystick Steering in Docking Situations .....	4
Figure 2 System Diagram .....	8
Figure 3 Body Reference Frame .....	12
Figure 4 Motor and Boat Geometry .....	16
Figure 5 LIAC Architecture .....	28
Figure 6 Surge Subsystem Reference Model Step Input Response .....	33
Figure 7 Sway/Yaw Subsystem Reference Model Step Input Response .....	34
Figure 8 Moment Arms as a Function of Steering Angle.....	39
Figure 9 Light Weight Narrow Motors Simulation.....	42
Figure 10 Light Weight Narrow Motors Simulation Parameter Estimates .....	43
Figure 11 Light Weight Wide Motors Simulation .....	43
Figure 12 Light Weight Wide Motors Simulation Parameter Estimates.....	44
Figure 13 Light Weight Wide Motors Simulation with Wind Disturbance .....	44
Figure 14 Light Weight Wide Simulation Parameter Estimates with Wind Disturbance	45
Figure 15 Heavy Weight Narrow Motors Simulation .....	46
Figure 16 Heavy Weight Narrow Motors Simulation Parameter Estimates.....	46
Figure 17 Heavy Weight Wide Motors Simulation .....	47
Figure 18 Heavy Weight Wide Motors Simulation Parameter Estimates .....	47
Figure 19 Test Tank .....	53
Figure 20 Sway Test Yaw Rate Results, All Scenarios.....	68
Figure 21 Sway Test Surge Velocity Results, All Scenarios.....	69
Figure 22 Yaw Test Position Error Results All Scenarios .....	69
Figure 23 Heavy Weight Wide Motors Fixed Nominal Power .....	71
Figure 24 Heavy Weight Wide Motors Modulated Nominal Power .....	71
Figure 25 Test Boat CAD Assembly.....	81
Figure 26 Test Boat CAD Assembly Wire Diagram.....	81

Figure 27 Full Scale Center Console Plywood Fishing Boat Construction ..... 82

Figure 28 Full Size Custom Center Console Boat Under Construction..... 82

Figure 29 Test Boat Hull ..... 82

## I. INTRODUCTION

### A. Background

Some recreational boaters say, “*You can’t buy happiness but you can buy a boat and that’s pretty close.*” Boaters love the prospect of being on the water with family and friends. They hope each trip is memorable and safe. However, at the end of the trip wind, current, and the complex nature of boat motion can conspire to make docking difficult. To make maneuvering close to the dock easier, marine engine manufacturers created alternative steering control systems. The alternative systems invite the captain to let go of the traditional wheel and throttle and grab a three-axis joystick controller. With the intuitive joystick, the captain can command the boat’s velocity vector and let the computer control the engines and steering mechanisms as required. Thus, the boaters’ happiness is hopefully restored even when facing stressful docking scenarios.

There are joystick control systems for all three main propulsion categories: pod drives, stern drives, and outboards. These propulsion systems are applied to as many boat categories as practical including: runabouts, express cruisers, and center console fishing boats. The target boats for joystick control typically have hulls which are stepped or non-stepped with anywhere between 18° to 30° dead rise. The boat weights can range from approximately 5,000 to 25,000 pounds and boat lengths can range from 24 to 48 feet (Lemancik, 2009). With the above target specifications, most multi-engine large planing boats can be equipped with joystick control.

Despite the variety in target boat hull design, all boats equipped with a joystick controller have essentially the same non-adaptive controller. The controller is designed to drive the actuators to calibrated set points under individual feedback control. For example, the control computer receives input from the joystick and sends open loop commands for throttle, shift, and steering angle based on the controller's calibration (Lemancik, 2009). This allows the captain to *twist* and/or *nudge* the joystick and enjoy astounding control while maneuvering. For the non-adaptive controller to work as expected, it is critical to calibrate the set points for each individual vessel.

Having to calibrate non-adaptive controls for each boat causes the manufacturer to deal with two undesirable conditions. For one, the cost of experimentally identifying and manually loading boat parameters in the field (not at the factory) is high and a potential bottleneck for sales. While recreational marine volumes are low compared to the automotive industry, relying on qualified field engineers to commission all boats limits the total number of boats which can be commissioned in each season. Another undesirable condition is the control's robustness. On large boats, the critical boat parameters will not change too much from voyage to voyage; however, on smaller boats this is not the case. Small boats are lighter; therefore, they are more sensitive to changes in weight due to the number of people and provisions onboard. Consequently, high volume markets, such as pontoon boats, are excluded.

The key question is, "Can the calibration process be eliminated through automation?" If so, the controller would have to either identify the system parameters or

identify the controller parameters automatically. The controller might then also be more robust. Can the current controller be replaced with an adaptive controller?

## B. Statement of the Problem

The opportunity to configure more boat classes with joystick controllers and to reduce the cost and time to commission existing boats with joystick controllers could come from creating a controller which does not require calibration. The controller would need to function without knowing the essential boat parameters such as: the distance between the engines and the center of lateral resistance, the distance between the engines and the center line, and the boat's inertial properties. These parameters will be described in more detail in Section II Physical and Mathematical Models below. For now, these are the parameters which define the boat to be controlled and how the actuators relate to the boat. A controller which could adapt to unknown parameters while providing exceptional control would solve the problem.

The key challenge is to adapt to the unknown parameters quickly and effectively. The adaptation should occur so quickly that it is not noticed by the captain. The captain will notice if the controller is not adapting because a controller error in one axis could lead to motion in another axis. For example, if the captain is trying to move laterally and the controller is not calibrated correctly, then the boat will rotate unintentionally. To avoid undesirable motion, the adaptive controller must adapt quickly to perform well in the critical slow-speed maneuvers.

### *Specific Performance Requirements for Two Critical Maneuvers*

In operation, the critical maneuvers for slow-speed maneuvering are stationary rotation (yaw) and pure translation (sway). Industry product marketing brochures from the two main competitors in the space, Mercury Marine (2014) and Volvo Penta (2016), make claims such as, “Push the joystick to port or starboard and your boat goes sideways. Even “impossible” berths are now accessible. Twist the top to rotate,” and “Rotate on its own axis with a twist of the joystick.” These two maneuvers in sequence would allow the captain to pull away from a pier side mooring and change direction within a single boat length shown in Figure 1.

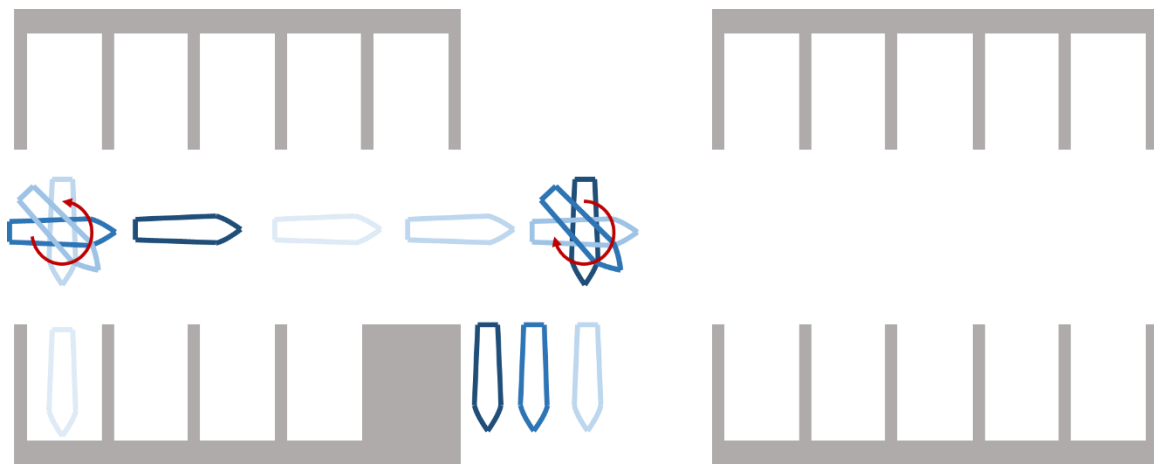


**Figure 1 Joystick Steering in Docking Situations**

Hence, the goal of the research was to create an adaptive boat controller which solves for the critical unknown parameters in a way that meets the following the requirements specified in Table 1.

**Table 1 Performance Requirements**

<b>Maneuver</b>		<b>Requirement</b>
1	Stationary Rotation (Pure Yaw)	Full 360° rotation without changing position by more than one boat length
2	Lateral Translation (Pure Sway)	Three beam width translation with less than 10° rotation or forward/aft translation

*Current State of the Problem*

Today, joystick control systems for recreational boats are electromechanical systems which employ a programmable controller to activate steering and thrust controls in a way that creates a net force and/or moment. As stated in Newton's second law, the acceleration of an object as produced by a net force is directly proportional to the magnitude of the net force, in the same direction of the net force, and inversely proportional to the mass of the object. This means that a boat should accelerate laterally if the net force at the center of mass in the fore/aft direction is zero, the net force at the center of mass in the port/starboard direction is greater than zero, and the net moment at the center of mass is zero. Similarly, a boat should accelerate in yaw if the net forces at the center of mass in all directions is zero and the net moment at the center of mass is greater than zero. To create the net force and moment vectors, the propulsion system must have two or more thrusters with independent steering, shift, and propeller speed control capability. With this capability, the thrust of each independent motor can be directed to create the desired force and/or moment.

To create the net force and moment, the boat can be modeled as a group of subsystems which operate together. A high-level system description, diagram (Figure 2), and table of system variables (Table 2) are provided below:

1. Hull – The boat hull provides buoyant force. The hull form determines the hydrodynamic forces. The hull geometry, materials, and load out (i.e., number of people onboard, supplies, etc. which can be variable) determine boats inertia matrix.
2. Motion sensors – The sensors measure accelerations and magnetic heading.
3. Controller – The controller receives the input from the joystick and calculates set points for individually controlled steering, shift, and thrust actuators.
4. Steering system – The steering system consists of independent mechanical rotation systems which rotate to aim the thrust vector on a desired angle.
5. Propulsion system – The propulsion system consists of independent mechanical rotation systems which change in speed and direction to generate the desired thrust force.
6. Ballast – The ballast compartments allow for internal mass to be added to the boat. In the test boat, the ballast compartments enable different inertia scenarios. In target applications, recreational boats accommodate different load-outs in terms of people and gear.
7. Boat power supply – The power supply provides the energy needed to drive the boat actuators and to power onboard sensors.
8. Motor-to-Motor distance mechanism – This mechanism enables different boat geometry scenarios (not present in target applications, only the test boat).
9. Disturbances – The controller faces disturbances in the form of wind, current, and waves which will impact the motion of the boat.

Current joystick systems can be described as open loop control with the human in the loop to adapt to disturbances and calibration errors. The controller commands the actuators to set points preset during the calibration process. The calibration process ensures the parameters loaded into the controller enable the subsystems to work together as desired. Application engineers identify boat parameters through research, measurement, and often on-water testing. After identifying the parameters, they are loaded into the control computer manually to drive the steering mechanism and engine speed to the proper settings (Lemancik, 2009). Consequently, the joystick control is

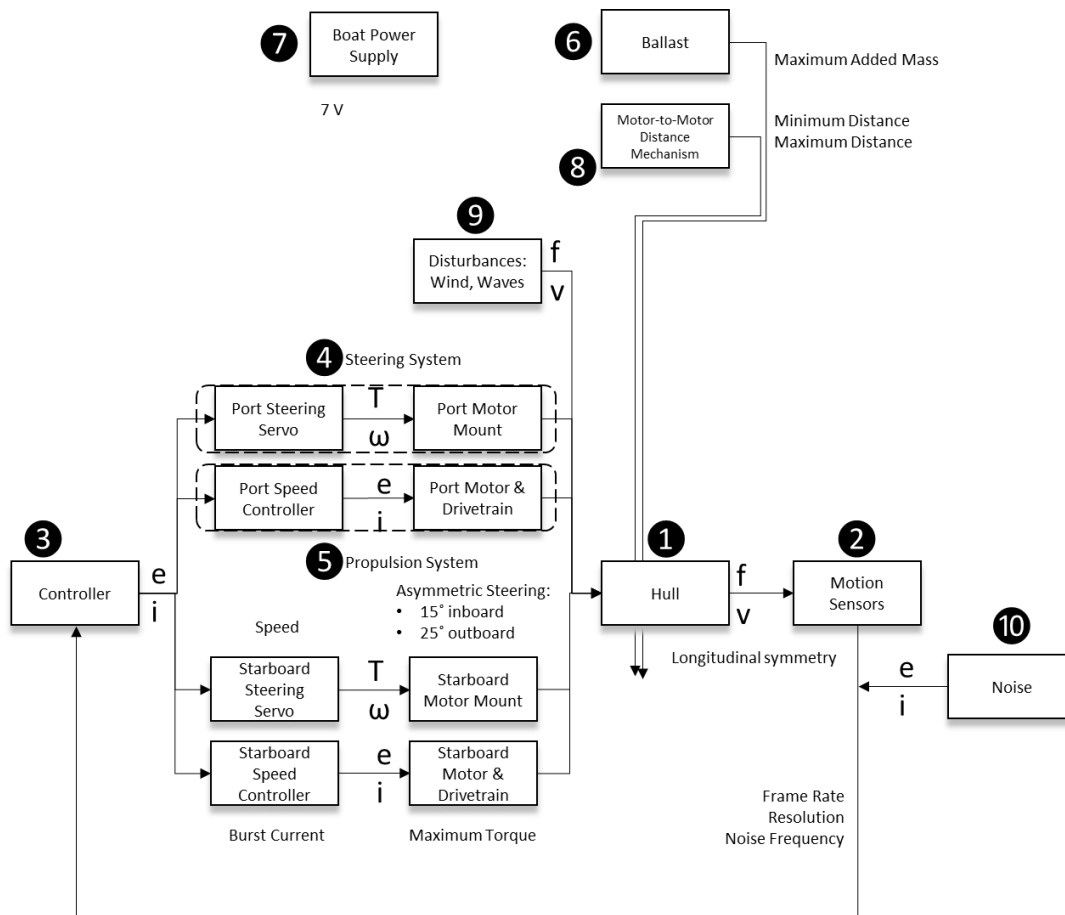


smooth and intuitive. However, as noted above, the system cannot adapt to changes in total weight or disturbances such as wind. In the presence of disturbances or calibration errors, the captain must modify the inputs to get the desired motion in today's integrated joystick systems. A fast-adapting system with high performance and disturbance rejection would eliminate the calibration process.

**Table 2 Through and Across Variables in the Joystick Control System**

<b>Variable</b>	<b>Definition</b>	<b>Description</b>
T	Torque	Moment applied to the rotating components (N-m)
$\omega$	Angular speed	Angular velocity of rotating components (rad/s)
f	Force	Linear force applied to system components (N)
v	Velocity	Linear velocity of system components (m/s)
e	Voltage	Electrical potential (Volts)
i	Electrical current	Electrical currents (Amp)

**Figure 2 System Diagram**



### C. Statement of the Procedure

#### *Overview*

The research was conducted through a model-based, systems engineering approach (Craig, 2012) outlined in Table 3. The key concept behind the approach is to follow a logical progression of steps where each step builds on the previous step to create new insight to the physical problem. The basic principle of the process was to start with

the physical system, apply first principles to identify the critical relationships, and then leverage mathematical modeling before beginning the hardware design and physical testing steps. In this research, the insights which shaped control development came from building the mathematic model (steps two through five) which will be described in detail below. As such, the approach was suitable for breaking down the inherent complexity of both boat motion and multidisciplinary mechanical systems.

**Table 3 Model Based Systems Engineering Approach**

Step	Name	Description
1	Physical System	The physical system is a scale model test boat which resembles joystick control target applications. Like the target applications, the test boat is a deep “v” shaped planing mono hull with a length to beam ratio of four and twenty-five-degree dead rise. The hull is symmetrical from bow to stern. Ballast compartments are incorporated into the hull to create different inertia scenarios. Also, the propulsion system is installed at the stern without bow thrusters such that the motors can be moved inboard and outboard to vary the propulsion system geometry. This enables scenarios varying engine to engine center distance or engine to center line distance.
2	Parameter Identification	The physical parameters were identified by direct measurement in most cases. Moments of inertia were estimated using CAD models in SolidEdge ST6.
3	Physical Model	The physical model was derived by leveraging several resources and by making simplifying assumptions outlined in the Physical and Mathematical Modeling section.
4	Mathematical Model	The mathematical model followed the physical model as outlined in the Physical and Mathematical Modeling section.

<b>Step</b>	<b>Name</b>	<b>Description</b>
5	Mathematical Analysis	The mathematical model was programmed in MATLAB. The mathematical model provided an opportunity to build insight from studying the input/output performance of the model and to iterate quickly in the controller design.
6	System Measurement	<p>The physical system was tested in two maneuvers in four scenarios each.</p> <p>Sway translation was also tested with a wind disturbance. The wind disturbance was created by a household fan blowing directly down the length of the test tank (beam-on).</p> <p>The performance of the physical system was measured through object tracking in digital video.</p>
7	Measurement Analysis	Measurement analysis of the physical system was completed in Microsoft Excel. The analysis compared the actual displacement against the original research design requirements.
8	Comparison of Predicted vs. Actual	The comparison of predicted vs. actual performance was completed qualitatively.
9	Design Assessment	After considering the measurement analysis and applying engineering judgment, design improvements were identified.
10	Design Changes	After analyzing the actual performance with the mathematical model, a new strategy for power was implemented in MATLAB

## II. PHYSICAL AND MATHEMATICAL MODELS

### A. Introduction

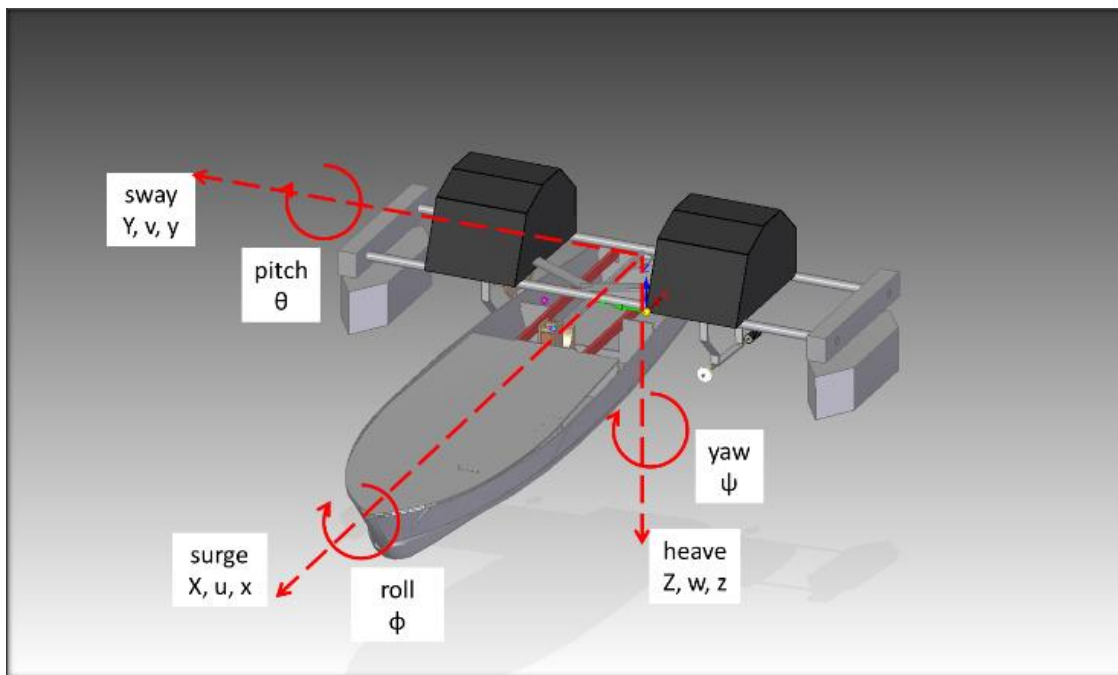
Through several simplifying assumptions described below, a mathematical model was derived from the full system of six coupled, nonlinear equations which describe boat motion (Fossen, 2011). The critical process in deriving the model was focusing on sway and rotation at very slow speeds. By focusing on the target maneuvers, a boat's motion can be treated as a rigid body under the forces of the propulsion system, the external environment, and (once moving) hydrodynamics. How these external forces act on the boat is a function of several factors such as the boat's shape, speed, the boat's center of gravity, and even the seaway boundaries (Tupper, 2004). After carefully considering the relative impact of these forces, judgment was applied to make the model as simple as possible and still provide insight suitable for simulation and control development.

### B. Reference Frames

The model followed the standard notation in Table 4 and Figure 3 as defined by Society of Naval Architects and Marine Engineers (SNAME) for all six degrees of freedom (Fossen, 2011).

**Table 4 Coordinate System**

DOF	Motion	Description	Forces and Moments	Linear and Angular Velocities	Positions and Angles
1	Surge	Linear motion bow to stern	X	u	x
2	Sway	Linear motion port to starboard	Y	v	y
3	Heave	Linear motion up and down	Z	w	z
4	Roll	Angular motion about the longitudinal axis	K	p	$\phi$
5	Pitch	Angular motion about the lateral axis	M	q	$\theta$
6	Yaw	Angular motion about the vertical axis	N	r	$\psi$

**Figure 3 Body Reference Frame**

### C. Rigid-Body Kinematics and Kinetics

The equations of motion for boats as rigid bodies can be derived using Newton-Euler or Lagrangian methods. With no constraints in linear or angular motion, a boat has six degrees of freedom. The generalized forces and moments on the boat are usually

modeled by using *maneuvering theory* or *seakeeping theory*. Maneuvering theory applies to boats, like the test boat, traveling at constant speeds in calm seas (Fossen, 2011).

In maneuvering theory, as in this research, the focus is on motion in the horizontal plane at slow speeds (surge, sway, and yaw). It is assumed that there are no waves; therefore, there is no motion in the vertical plane (no heave, roll, or pitch). Without rolling, heaving, and pitching motions, the equations of motion are reduced to three coupled degrees of freedom (Fossen, 2011):

$$X = m(\dot{u} - \dot{\psi}v - x_G\dot{\psi}^2) \quad (1)$$

$$Y = m(\dot{v} + u\dot{\psi} + x_G\ddot{\psi}) \quad (2)$$

$$N = I_z\ddot{\psi} + mx_G(\dot{v} + u\dot{\psi}) \quad (3)$$

where  $X$ ,  $Y$ , and  $N$  are the sum of the forces and moments acting on the boat in the body reference frame with the origin at the transom on the boat's centerline.

The generalized forces acting on the boat can be organized into four groups:

1. control forces,
2. hydrodynamic added mass,
3. damping, and
4. wind forces.

For this research, the critical group is the control forces group. The control forces are generated by the actuators for steering and thrust. They put the boat into motion. Once in motion, the boat forces the water in its path to flow around the hull. This flow

generates the second most important group known as hydrodynamic added mass which can be characterized as inertial forces. The inertial forces are caused by the boat physically moving the water around the hull (Misra, 2008). The third group, hydrodynamic damping force, is caused by skin friction and lift forces as the water flows around the boat. As such, the hydrodynamic added mass and damping forces are a function of the hull form (Misra, 2008). Because the boat is symmetrical along the longitudinal axis, moving forward at very slow speeds, surge is assumed to be decoupled from sway and yaw. Unlike the longitudinal axis, the shape of the hull along the lateral axis is asymmetric. The asymmetric shape along this axis causes asymmetric flow around the hull in sway and yaw motions. Hence, motion in these two directions are coupled. The implication of the above is that hydrodynamic forces develop when the ship is moving as a function of velocity and acceleration. For surge motion, the forces are a function of surge velocity and surge acceleration only. For sway and yaw motion, the forces are coupled such that motion in either state will generate forces as function of surge and sway velocity and acceleration (Misra, 2008). The relationships between motion and hydrodynamic forces are nonlinear across a wide speed or acceleration range. However, it is assumed that at low speeds the hydrodynamic derivatives can be linearized around the target speeds such that the hydrodynamic forces,  $\mathbf{u}_{hyd}$ , can be expressed using SNAME notation as:

$$\mathbf{u}_{hyd} = \begin{bmatrix} uX_u + \dot{u}X_{\dot{u}} \\ vY_v + \dot{v}Y_{\dot{v}} + rY_r + \dot{r}Y_{\dot{r}} \\ vN_v + \dot{v}N_{\dot{v}} + rN_r + \dot{r}N_{\dot{r}} \end{bmatrix} \quad (4)$$



The fourth group is the wind. The wind creates an airflow over the hull which creates a pressure field on the boat above the waterline. Together, the generalized forces were modeled as a control force, additional inertia and damping forces, and a disturbance force respectively.

As a control force, the thrust forces came from two independent propulsion systems to direct thrust. For this research, the thrust magnitude was assumed to be a linear function of motor speed. Fossen (2011) recommends a nonlinear propeller torque and thrust model which varies as a function of vessel speed. However, in this research the control objective does not require precise thrust control but rather precise thrust vector control. Therefore, the propeller was assumed to be an ideal transformer which transforms rotational mechanical energy into translational mechanical energy without energy storage, cavitation (slipping), or dissipation. That is, the angular speed and torque about the propeller shaft will be converted to translation about an axis fixed to the propeller shaft and force about the same axis at a gain proportional to the propeller pitch – like a rack and pinion gear.

The thrust direction was assumed to follow commanded steering angles as a first order servo system for this research. By observation, the servo responded to commands about as fast as the controller's discrete time step which was much faster than the hull settling time; therefore, modeling the steering system as a second order servo system would have unnecessarily complicated the research. The propulsion systems were integrated with the boat such that each system was equidistant from the centerline; however, the distance to centerline could be changed to test the controller. Also, the boat

ballast could be changed which changed the distance between the propulsion systems and the center of gravity as depicted in Figure 4. The net force and moment the propulsion systems created are a function of the propeller speed, steering angle, distance between the system and centerline, and distance between the system and the center of gravity.

Let  $\mathbf{u}_{thr}$  be the vector of forces and moments generated by the propulsion systems in surge, sway, and yaw respectively such that:

$$\mathbf{u}_{thr} = \begin{bmatrix} u_{thr1} \\ u_{thr2} \\ u_{thr3} \end{bmatrix}. \quad (5)$$

Further let:

$F_1 =$  thrust generated by the port engine

$F_2 =$  thrust generated by the starboard engine

$\delta_1 =$  port engine steering angle

$\delta_2 =$  starboard engine steering angle

$N_1 =$  moment about z generated by the port engine

$N_2 =$  moment about z generated by the starboard engine

$B =$  distance from vessel centerline to the motor mount

$L =$  distance from center of rotation to the motor mount

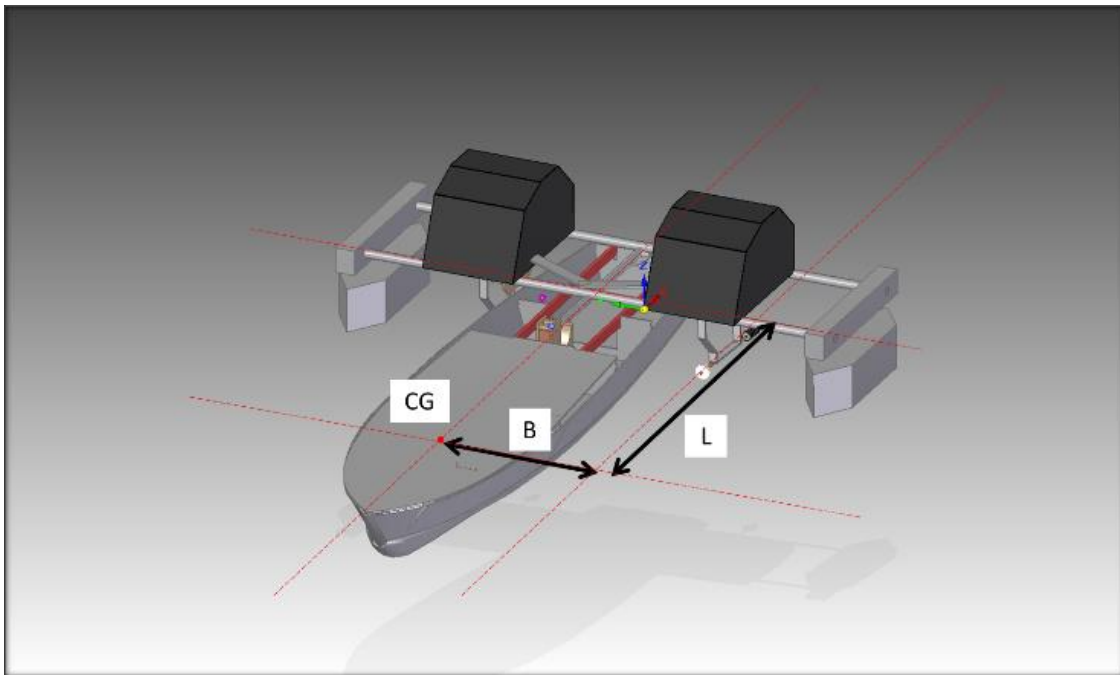


**Figure 4 Motor and Boat Geometry**

From inspection, the propulsive forces and moments at the center of mass from each system can be written in vector notation as:

$$\vec{F}_1 = F_1 \cos \delta_1 \hat{x}_b + F_1 \sin \delta_1 \hat{y}_b \quad (6)$$

$$\vec{F}_2 = F_2 \cos \delta_2 \hat{x}_b + F_2 \sin \delta_2 \hat{y}_b \quad (7)$$

$$\vec{N}_1 = (-LF_1 \sin \delta_1 - B F_1 \cos \delta_1) \hat{z}_b \quad (8)$$

$$\vec{N}_2 = (LF_2 \sin \delta_2 + B F_2 \cos \delta_2) \hat{z}_b \quad (9)$$

Then, the net forces and moments can be written as:

$$u_{thr1} = F_1 \cos \delta_1 + F_2 \cos \delta_2 \quad (10)$$

$$u_{thr2} = F_1 \sin \delta_1 + F_2 \sin \delta_2 \quad (11)$$

$$u_{thr3} = L(F_2 \sin \delta_2 - F_1 \sin \delta_1) + B(-F_1 \cos \delta_1 + F_2 \cos \delta_2) \quad (12)$$

As will be described in Section III Control Strategy in more detail, it was assumed the control strategy would dictate that the steering angles of the two systems be equal and opposite such that:

$$\delta_2 = \pi - \delta_1 \quad (13)$$

Note that the propellers can be driven in forward or reverse which would orient the thrust vector forward or aft accordingly. So, the equations above can be simplified to:

$$u_{thr1} = \cos \delta_1 (F_1 - F_2) \quad (14)$$

$$u_{thr2} = \sin \delta_1 (F_1 + F_2) \quad (15)$$

$$u_{thr3} = L \sin \delta_1 (F_1 + F_2) - B \cos \delta_1 (F_1 + F_2) \quad (16)$$

Therefore, the force from the propulsion system,  $\mathbf{u}_{prop}$ , was modeled as:

$$\mathbf{u}_{prop} = \begin{bmatrix} \cos \delta_1 (F_1 - F_2) \\ \sin \delta_1 (F_1 + F_2) \\ L \sin \delta_1 (F_1 + F_2) - B \cos \delta_1 (F_1 + F_2) \end{bmatrix}. \quad (17)$$

The added mass hydrodynamic derivatives  $Y_{\dot{v}}$  for sway is critical to control in the pure sway maneuver. When the boat moves laterally, it must displace the water in the boat's path. The boat pushes a mass of water like the mass of the boat around the hull. Put another way, a sway force from the boat controls will meet an opposing force from the water's inertia. The opposing force can be thought of as a pressure field whose shape reflects a longitudinal cross-section of the hull below the waterline (Misra, 2008). The net force is an integration of the pressure field over the length of the hull.

$$\text{Added Mass Force} = C_d \rho V^2 A / 2 \quad (18)$$

Where

$$\begin{aligned} C_d &= \text{coefficient of drag} \\ \rho &= \text{water density} \\ V^2 &= \text{velocity squared} \\ A &= \text{surface area perpendicular to the flow} \end{aligned}$$

The point on the hull at which the net force acts is referred to as the center of lateral resistance (COLR). Therefore, for pure sway motion, the net force vector from the actuators must act on the COLR.

Finally, the experiments assumed no wind and no current. However, wind was created as a disturbance to test the controller in some scenarios. The force of the wind was expressed simply as  $\mathbf{u}_{dist}$ .

Before bringing the model of the forces together with the rigid body equations, the assumptions made to the forces were also applied to the rigid body equations. The

slow speed assumptions made to linearize the hydrodynamic forces were applied to the rigid body equations. The initial velocities are all zero:

$$u_i = 0; v_i = 0; r_i = 0$$

The accelerations were expected to be very small values:

$$\dot{u} < 0.1 \text{ m/s}^2; \dot{v} < 0.1 \text{ m/s}^2; \dot{r} < 3 \text{ degrees/s}^2$$

Also, the assumption was made that the slow speeds decouple surge from sway and yaw.

Finally, it was assumed that the center of gravity would lie on the boat's centerline.

Therefore,

$$X = m(\dot{u} - \dot{\psi}v - x_G\dot{\psi}^2) \cong m(\dot{u} - x_G\dot{\psi}^2) \quad (19)$$

$$Y = m(\dot{v} + (U_i + du)\dot{\psi} + x_G\ddot{\psi}) \cong m(\dot{v} + x_G\ddot{\psi}) \quad (20)$$

$$N = I_z\ddot{\psi} + mx_G(\dot{v} + (U_i + du)\dot{\psi}) \cong I_z\ddot{\psi} + mx_G(\dot{v}) \quad (21)$$

Which implies

$$X = m(\dot{u} - x_G\dot{\psi}^2) = uX_u + \dot{u}X_{\dot{u}} + \cos \delta_1(F_1 - F_2) \quad (22)$$

$$Y = m(\dot{v} + x_G\ddot{\psi}) = vY_v + \dot{v}Y_{\dot{v}} + rY_r + \dot{r}Y_{\dot{r}} + \sin \delta_1(F_1 + F_2) \quad (23)$$

$$\begin{aligned} N &= I_z\ddot{\psi} + mx_G(\dot{v}) \\ &= vN_v + \dot{v}N_{\dot{v}} + rN_r + \dot{r}N_{\dot{r}} + (F_1 + F_2)(L\sin \delta_1 - B\cos \delta_1) \end{aligned} \quad (24)$$

The above equations can be rewritten in matrix format as follows:

$$\begin{bmatrix} m-X_{\dot{u}} & 0 & 0 \\ 0 & m-Y_{\dot{v}} & mx_g-Y_{\dot{r}} \\ 0 & mx_g-Y_{\dot{r}} & I_z-N_{\dot{r}} \end{bmatrix} \begin{bmatrix} \dot{u} \\ \dot{v} \\ \dot{r} \end{bmatrix} + \begin{bmatrix} -X_u & 0 & 0 \\ 0 & -Y_v & -Y_r \\ 0 & -N_v & -N_r \end{bmatrix} \begin{bmatrix} u \\ v \\ r \end{bmatrix} = \begin{bmatrix} \cos \delta_1(F_1 - F_2) \\ \sin \delta_1(F_1 + F_2) \\ (B\sin \delta_1 - L\cos \delta_1)(F_1 + F_2) \end{bmatrix} \quad (25)$$

After analyzing each factor in the full state space equations, the simplifying assumptions above justified the use of a three degree of freedom model in which surge was decoupled from sway and yaw. The critical assumptions included treating the boat as a rigid body symmetrical along the centerline, maneuvering at slow speed in calms seas with no wind. It is important to note that each of the above values will be unknown

to the controller except for  $F_1$  and  $F_2$ . With the simplifying assumptions having been made, the model was ready for simulation and control development.

### III. CONTROL STRATEGY

#### A. Introduction

Today's joystick control systems require a manual calibration process because the current strategy relies on classical control techniques for controlling subsystems while the overall boat control is left to the captain. In the outer loop of the boat, the captain makes continuous changes to the joystick input until the desired trajectory is achieved. In the inner loop, the shift, throttle, and steering commands are essentially set points (under PID control). The set points are calibrated during the manual configuration mentioned above (Lemancik, 2009). The current strategy works for boaters because it is very intuitive. If the boat yaws left un-commanded, the captain twists the joystick to the right to compensate. Within the control system, the joystick inputs drive the subsystem components to set points derived during the system calibration. The individual subsystem controllers use classical design techniques to meet performance expectations (Lemancik, 2009). Therefore, to eliminate the manual calibration process, the controller must replace the human in the outer loop by adapting to changes or errors in the vessel calibration and/or disturbances.

#### B. Adaptive Control Historical Perspective

There are several classes of marine vessel controls. Controls for set point regulation (i.e., heading, speed, trim angle, etc.) are *autopilots*. Controls for waypoint tracking, trajectory tracking, or path following are *guidance systems*. Controls for minimizing undesirable motion (i.e., rolling) are *stabilizers*. Controls for maintaining a

vessel's position and heading exclusively through thrusters and main propellers are *dynamic positioning* (DP) controllers (Fossen, 2011).

The integrated joystick systems in recreational boats are DP controls. However, traditional DP applications include mobile offshore drilling vessels, research vessels, and cruise ships. Each vehicle example above are built as capital projects produced at low volume. In these situations, the DP control architecture is designed as an integrated subsystem (Fossen, 2011) during the mechanical design or after each of the critical parameters are largely known. The difference between traditional DP design and joystick control design for recreational boats is that for boats, joystick control is an add-on option. The option is meant to be available with as many different boat designs as possible. As described in Section I Introduction above, the joystick controller is tuned for each individual boat which creates cost and capacity problems. If the joystick maker is going to avoid individual boat calibrations, then the controller will have to leverage adaptive control techniques.

Adaptive control has a long, progressive history. In the early 1950's, aerospace programs required advances in adaptive control to enable autopilots to perform over new, larger ranges of altitudes and airspeeds. The new requirements disqualified fixed gain controllers. In response, new adaptive controllers used gain scheduling based on a variety of measured conditions such as aircraft altitude and Mach number. In search of greater performance, controllers were developed using self-adjustment following the MIT rule or sensitivity rule.



The next advances came in increased robustness. By the 1970's Lyapunov based stability was introduced. As a reference, several variations of MRAC are available for study in general (Annaswamy, 1989) as well as applications to vessel dynamic positioning in particular (Verma, 2004). In marine control, the first DP controls were implemented in the 1960's using decoupled PID for surge, sway, and yaw. By the late 1970's, more refined DP controllers were implemented using linear optimal theory and Kalman filters for better performance (Hovakimyan, 2010).

By the 1990's, controllers attacked nonlinear control with several methodologies. DP controllers have used model reference adaptive control (MRAC) variations of PID and LQR controls as well as more advanced techniques such as integrator back stepping (Fossen, 2011). By the 2000's, engineers investigated search methods, multiple models, and more sophisticated switching techniques. Similarly, there exist several strategies for LQR and integrator back stepping for dynamic positioning (Fossen, 2011) and heading control (Jouffroy, 2012). Over the last sixty years, adaptive control provided strategies to overcome parametric uncertainties under several classes of control problems.

Nonetheless, the control theory developed over the last sixty years to create adaptive controllers have limitations (Anderson, 2005). All adaptive controls were limited to slow varying uncertainties and required persistent excitation. When the controller had to have fast adaption, the actuators faced high frequency oscillations in the control signal which reduced the system's tolerance to time delay.

### C. Adaptive Joystick Control Problem Detail

The adaptive control problem for the recreational joystick is different from adaptive DP controls in the shipbuilding industry, marine autopilots, or even aerospace flight controls because of a unique combination of factors. As listed in Table 5, the controller has neither an actuator dedicated to yaw, knowledge of the actuator's neutral yaw rate position, nor persistent excitation. If the controller had to overcome just one of the above factors, the controller could be designed in a straightforward process.

One of the contributing factors is the lack of a dedicated yaw rate actuator. While there are boats with bow or stern thrusters dedicated to yaw rate, installation typically requires cutting holes into the hull. Marine engine manufacturers can provide the same controllability without the cost and risk of modifying the hull. If the boat has two or more main engines, then the boat is over actuated. That is, the boat has three degrees of freedom (surge, sway, and yaw) and two engines with controllable steering angles and thrust (magnitude and direction) for a total of four independent inputs. Since the number of inputs is greater than the system's degrees of freedom, the controls can be allocated using multiple strategies.

The other contributing factor, the fundamental issue which creates the cost and complexity in commissioning today's recreational joystick controls, is the variability in the location of the COLR. This is critical because to execute pure translation maneuvers (zero yaw rate) the controller must command steering angles to direct the force vector through the COLR. Unlike common DP and autopilot controls which adapt to an

unknown magnitude of the actuator gain with a known sign (Fossen, 2011), the recreational boat joystick controller does not know the neutral position of the yaw actuator. In common autopilots, when the rudder is placed at a neutral angle it will not apply a moment to the boat, assuming no trim is needed. When the rudder is turned to the right of center, the rudder will apply a clockwise moment. When the rudder is turned to the left, the rudder will apply a counter-clockwise moment center. In common DP control which use bow or stern thrusters, the moment direction is created by the direction of the thruster's propeller rotation – one way for clockwise, the other way for counter-clockwise. In the research case, the yaw control is provided by creating a moment through the placement of a net force vector relative to the COLR. To function, the recreational joystick control must adapt in finding the steering angle for the neutral position (while translating in sway).

Finally, the controller must adapt quickly without persistent excitation. The boat motion under joystick control should be smooth, slow, and precise. Often the wind and water will be calm in protected harbors. In contrast, adaptive DP controls and autopilots using model reference adaptive control assume the vessel is responding to wave and wind forces and/or moving at a constant forward speed which will provide the excitation needed to identify system parameters. Therefore, the lack of persistent excitation prohibits the use of traditional direct or indirect MRAC.

Each of the factors above in isolation have been overcome in different scenarios. What is unique is the combination of factors facing the recreational boat joystick controller. For example, if the COLR was unknown but there was a dedicated yaw rate

actuator (with or without persistent excitation), the system could use traditional linear feedback control techniques. For another, if the COLR was known and there was persistent excitation, then MRAC could be used. To overcome the combination of unique factors (Table 5) which impede adaptive control for joystick steering in recreation boats, the controller design required an innovative approach.

**Table 5 Factors in Controlling Recreation Boats with a Joystick**

<b>Factors in Controlling Recreation Boats with a Joystick</b>
<ul style="list-style-type: none"> <li>• Lack of a dedicated yaw rate control actuator in the presence of couple yaw/sway motion</li> <li>• Unknown center of lateral resistance</li> <li>• Lack of persistent excitation</li> </ul>

#### D. L1 Adaptive Control

The gateway innovation for this research came from the aerospace industry where a new approach to adaptive control was created. Through the late 1990's aerospace control systems for Boeing's X-36 and JDAM programs achieved performance targets by switching between hundreds of individual MRAC adaptive controllers (Hovakimyan, 2010). In traditional MRAC, the control objective is for the plant to follow the desired response. The tracking error is bounded by the magnitude of the adaptive gain. However, increasing the adaptive gain reduces system robustness. Therefore, switching from one adaptive controller to another based on Mach number, altitude, or other factors was a viable strategy for overcoming the tradeoff. Though viable, the cost and time of developing such complex switching adaptive controllers was deemed problematic (Anderson, 2005).

The features of the traditional MRAC architecture which are problematic for the aerospace applications above are the same features which make the architecture unusable for joystick steering in recreational boats. A traditional MRAC control system strives to improve speed of adaption and steady state tracking performance by adjusting either adaptive parameters in the controller or through direct system identification in the state predictor. In MRAC, the control objective is formulated as follows:

$$\dot{x}(t) = A_m x(t) + b(u(t) + \theta^T(t)x(t)), x(0) = x_0 \quad (26)$$

$$y(t) = c^T x(t) \quad (27)$$

Where

$A_m = \text{plant model}$

$\theta(t) = \text{vector of unknown plant parameters}$

$b, c = \text{vector of known actuator and output gains}$

$x, u, \text{ and } y = \text{state, input, and output respectively}$

The nominal MRAC controller is then defined as:

$$u_{MRAC} = -\theta^T(t)x(t) + k_{gr}r(t) \quad (28)$$

Where

$k_{gr} = \text{feedforward gain}$

$r = \text{desired output}$

By substitution, such that the plant will follow the desired reference system as follows:

$$\dot{x}_{des} = A_m x_{des}(t) + b k_{gr} r(t) \quad (29)$$

As shown, the nominal MRAC controller endeavors to cancel all uncertainties by identifying unknown parameters perfectly. Analysis of the nominal controller shows that there is an inverse relationship between performance and robustness and that persistent excitation of the system is required to achieve fast adaptation (Annaswamy, 1989). This is because the error between the predicted and measured state is used to adjust the

adaptive parameters in the state predictor or the controller (depending on the method used) which means the oscillations in the adaptive parameter estimates are passed into the control signal. To work around the above trade off, the aerospace applications switched from one MRAC controller to another as appropriate. For more practical controller development and implementation, new teams reformulated the adaptive control problem in a way which could be used to overcome the three main factors listed in Section III Control Strategy.

The new approach, L1 Adaptive Control (L1AC), redefined the control objective in a way that decoupled fast adaption from robustness. L1AC redefined the objective to only cancel uncertainties within a low frequency bandwidth of the control channel by placing a low pass filter between the Control Law and the Actuators as well as the State Predictor as shown in Figure 5.

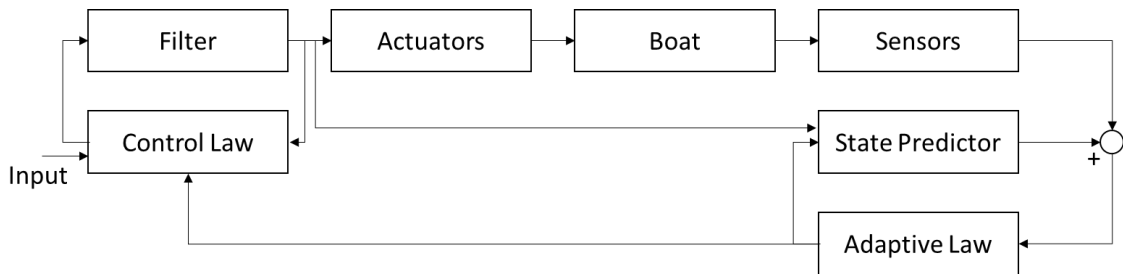


**Figure 5 L1AC Architecture**

Mathematically, the L1AC controller can be defined as:

$$u_{L1AC} = C(s)\{-\theta^T(t)x(t) + k_{gr}r(t)\} \quad (30)$$

Where

$C(s) = \text{transfer function of the low pass filter}$

Such that the plant will follow the desired reference system as follows:

$$\dot{x}_{ref} = A_m x_{ref}(t) + b\{(1-C(s))\theta^T x_{ref}(t) + C(s)k_{gr}r(t)\} \quad (31)$$

The filter thereby separates *parameter estimation* from *control*. Hokaimyan (2010) provides a thorough mathematical proof of L1AC controller's stability, bounded control input, and bounded state error. Hence, L1AC controllers enjoy several features listed in Table 6 such as fast adaption, without persistent excitation, for unknown parameters (i.e., actuator gain) without impacting performance (Hovakimyan, 2010).

As its chief advantage over MRAC in the joystick boat application, L1AC's fast adaption without persistent excitation creates value in two ways. For one, from the captain's perspective, the filter prevents the controller from driving the steering angle and engine power into high frequency oscillations. High frequency oscillations might cause the captain to lose confidence in the system or to feel concerned about mechanical wear. For another, the architecture creates an opportunity to overcome the core challenge of adapting quickly to the combined unknown actuator gain, unknown actuator sign, and the lack of a dedicated yaw rate control. Section E Designing the L1 Adaptive Control for the Test Boat will outline in detail the method used in this research.

Upstream of the Control Law, the Adaptive Laws revise model estimates such that the state error approaches zero. In addition to the adaptation of unknown plant parameters, the L1AC architecture can also adapt to unknown actuator gains and disturbances such that the full problem can be formulated as:

$$\dot{x}(t) = A_m x(t) + b(\omega u(t) - \theta^T(t)x(t) + \sigma), x(0) = x_0 \quad (32)$$

$$y(t) = c^T x(t) \quad (33)$$

Where

$A_m$  = matrix specifying the desired closed – loop system performance  
 $\omega, \sigma(t), \theta(t)$  = vector of unknown parameters within a known set  
 $b, c$  = known vectors  
 $x, u,$  and  $y$  = state, input, and output respectively

The Adaptive Laws use a projection operator, which requires a minimum and maximum value for each adaptive parameter, so that the adaptive estimates remain within the allowable range (Hovakimyan, 2010). Then, the projection is amplified by a fixed gain to calculate the rate of change in the estimate (please note that the hat symbol here is used to denote an estimate of the adaptive parameter):

$$\hat{\theta}(t) = \Gamma Proj(\hat{\theta}(t), -\tilde{x}^T(t)Pbx(t)) \quad (34)$$

$$\hat{\sigma}(t) = \Gamma Proj(\hat{\sigma}(t), -\tilde{x}^T(t)Pb) \quad (35)$$

$$\hat{\omega}(t) = \Gamma Proj(\hat{\omega}(t), -\tilde{x}^T(t)Pbu(t)) \quad (36)$$

Where

$\hat{\theta}$  = change in estimated value of  $\theta$  (unknown system parameter)  
 $\hat{\sigma}$  = change in estimated value of  $\sigma$  (unknown noise)  
 $\hat{\omega}$  = change in estimated value of  $\omega$  (unknown actuator gain)  
 $\Gamma$  = adaptive gain  
 $P$  = symmetric matrix such that  $P = P^T > 0$   
and solves a Lyapunov equation for stability  
 $\tilde{x}$  = state error (defined below)  
 $Proj$  = projection operator

It is the Adaptive Laws which help the controller drive the state error to zero in the face of uncertainties. In this research, the unknown system parameters include the mass matrix and hydrodynamic derivatives described in the mathematical model section above. The uncertain system input gains include the moment arms of the propulsion systems as



well as reverse propeller efficiency. The disturbances include forces from wind, waves, and currents. Therefore, the adaptation promises to deliver the research goal: eliminate the need for a bespoke calibration for each individual boat and to provide the boat a means to adapt to disturbances and/or changes.

Finally, as shown in Figure 5, upstream of the Adaptive Law is the State Predictor. The State Predictor calculates the reference model state as a function of the current adaptive variable estimates, the current measured states, and the reference model: and the error between the predicted and measured values:

$$\hat{\hat{x}}(t) = A_m \hat{x}(t) + b(\hat{\omega}(t)u(t) + \hat{\theta}^T x(t) + \hat{\sigma}(t)) \quad (37)$$

$$\hat{y}(t) = c^T \hat{x}(t) \quad (38)$$

Where

$$\begin{aligned} \hat{x} \text{ is the state estimate, } & \hat{x}(0) = x_0, \\ \hat{\theta} \text{ is the plant parameter estimate, } & \hat{\theta}(0) = \theta_0 \\ \hat{\omega} \text{ is the actuator gain estimate, } & \hat{\omega}(0) = \omega_0 \\ \hat{\sigma} \text{ is the disturbance estimate, } & \hat{\sigma}(0) = \sigma_0 \end{aligned}$$

Then, the State Predictor calculates the difference, or error, between the predicted state value and the measured value:

$$\tilde{x} = \hat{x} - x \quad (39)$$

Where

$$\tilde{x} = \text{state estimation error}$$

This is an essential piece of the adaptive control because the error,  $\tilde{x}$ , becomes the basis of the adaptive calculations. The chief advantage of the state predictor is that it allows the designer to choose a reference model with the desired closed loop dynamics. While there are considerations to be made in choosing the reference model, if the reference

model is close to the actual boat, then one L1 Adaptive Control state predictor might be used for each class of boat.

**Table 6 L1 Adaptive Control Features**

<b>L1 Adaptive Control's Main Features (Hovakimyan, 2010)</b>
<ul style="list-style-type: none"> <li>• Guaranteed fast adaption</li> <li>• Decoupled adaption and robustness</li> <li>• Guaranteed transient performance</li> <li>• Guaranteed time delay margin</li> <li>• Uniform scaled transient response dependent on the initial condition, value of the unknown parameter, and reference input</li> </ul>

As listed in Table 6, the L1AC architecture has features which uniquely meet the requirements for the research. The controller drives the plant to perform as the reference model. The critical process is feeding the parameter updates into the state predictor at a very high frequency while filtering that fast adaption signal in the control law. By so doing, L1AC overcomes the need for persistent excitation and offers an opportunity to adapt to the unknown actuator gain and disturbances.

#### E. Designing the L1 Adaptive Control for the Test Boat

The first step in designing the controller was to define the L1AC reference boat model. The reference model was defined such that the controller would drive the test boat scenarios to acceptable performance levels. Although somewhat arbitrary, it was assumed that if the surge subsystem adapted within three seconds the performance would be acceptable. Shorter adaption times are possible but would require higher performance in the subcomponents throughout the test boat systems. For example, faster adaption could be achieved with more refined steering control, a faster processor, a larger

propeller, and a higher performing sensor. After a brief trial in MATLAB, the following reference boat model was selected for surge:

$$\text{Surge subsystem } A_m = [-1.4]$$

With a surge subsystem reference model  $A_m = [-1.4]$ , the reference model would behave as boat with a ratio of drag coefficient to a total mass = -1.4. At this value, the reference subsystem's open loop response to a unit step input met the performance guideline as shown in Table 7 and Figure 6.

**Table 7 Surge Subsystem Reference Model Step Input Response**

State	Input	Rise Time	Peak Response	Settling Time
Surge Velocity	Surge Force	1.57 s	0.71 m/s	2.79 s

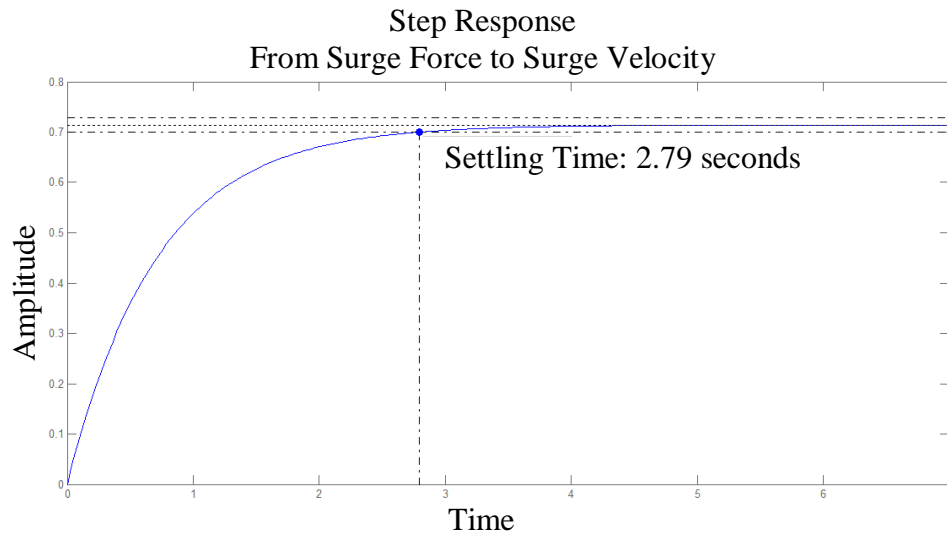


**Figure 6 Surge Subsystem Reference Model Step Input Response**

The approach for the sway-yaw subsystem was similar to the surge subsystem; however, the acceptable settling time was assumed to be six seconds. The following reference boat model was selected for sway/yaw:

$$\text{Sway - Yaw subsystem } A_m = \begin{bmatrix} 0 & -1 \\ 1 & -1.4 \end{bmatrix}$$

The reference model's response to a step input can be characterized as follows in Table 8 and Figure 7:

**Table 8 Sway/Yaw Subsystem Reference Model Step Input Response**

State	Input	Rise Time	Peak Response	Settling Time
Sway Velocity	Sway Force	1.56 s	1.5 m/s	5.27 s
	Yaw Moment	2.13 s	-1.05 m/s	5.98 s
Yaw Rate	Sway Force	2.13 s	1.05 rad/s	5.98 s
	Yaw Moment	0.00 s	0.46 rad/s	7.09 s

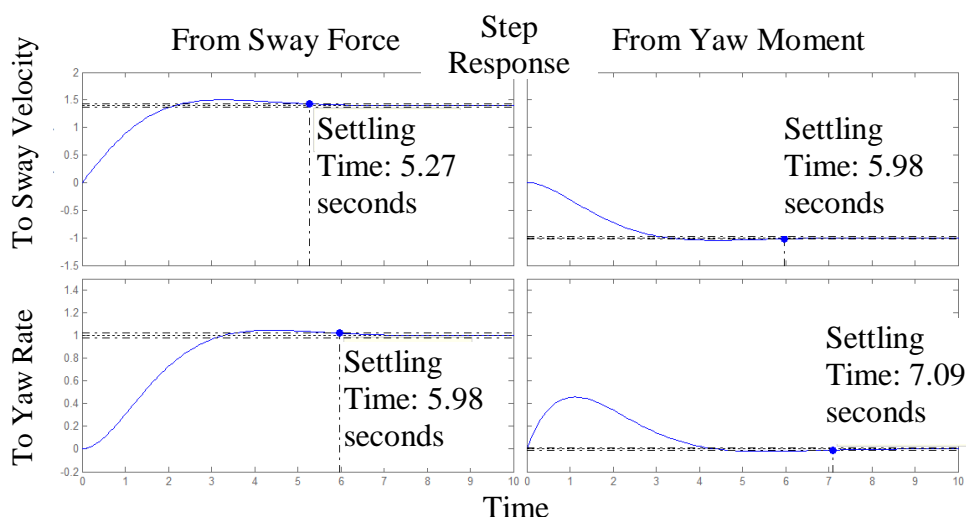


**Figure 7 Sway/Yaw Subsystem Reference Model Step Input Response**

Under the L1AC methodology, the state error is used to identify the adaptive parameters and to adjust the controller such that the predicted state follows the commanded state. By driving the test boat to the above reference model performance, it was predicted the test boat would perform well.

With the reference model defined, the state predictor and control law had to be designed such that the controller could overcome the key design challenge for the joystick control problem – unknown actuator gain and unknown sign. The critical step in the design process was creating a strategy to allocate actuators to each degree of freedom

and then to leverage the adaptive gains for each unknown. The actuators were allocated based on insight from the mathematical model. As outlined above, the mathematical model of the boat:

$$\begin{bmatrix} m-X_{\dot{u}} & 0 & 0 \\ 0 & m-Y_{\dot{v}} & mx_g-Y_{\dot{r}} \\ 0 & mx_g-Y_{\dot{r}} & I_z-N_{\dot{r}} \end{bmatrix} \begin{bmatrix} \dot{u} \\ \dot{v} \\ \dot{r} \end{bmatrix} + \begin{bmatrix} -X_u & 0 & 0 \\ 0 & -Y_v & -Y_r \\ 0 & -N_v & -N_r \end{bmatrix} \begin{bmatrix} u \\ v \\ r \end{bmatrix} = \begin{bmatrix} \cos \delta_1 (F_1 - F_2) \\ \sin \delta_1 (F_1 + F_2) \\ (B \sin \delta_1 - L \cos \delta_1) (F_1 + F_2) \end{bmatrix}$$

had to be restated to follow Hovakimyan's L1AC form:

$$\dot{x}(t) = A_m x(t) + b(\omega u(t) - \theta^T(t)x(t) + \sigma), x(0) = x_0 \quad (40)$$

$$y(t) = c^T x(t) \quad (41)$$

Where

$A_m =$  desired dynamics  
 $b =$  known constant matrix  
 $u =$  control input  
 $\omega =$  unknown constant with known sign  
 $\theta =$  unknown vessel parameters  
 $\sigma = 0$  (no wind, no current, no waves)  
 $y =$  output

To accomplish this, the mathematical model was reformatted to align with the L1AC formulation.

Once the mathematical model was in the standard L1AC form, decisions must be made to allocate the actuators because the boat is over-actuated. There are more independent actuators (four) than degrees of freedom (three). The four actuators are:

1. Port motor steering angle
2. Starboard motor steering angle
3. Port motor thrust vector (forward/reverse plus magnitude)
4. Starboard motor thrust vector (forward/reverse plus magnitude)

Therefore, to simplify the control strategy, one of the actuators was virtually constrained. For the final control design, the controller constrained the steering angles for the two motors to always be equal and opposite for two reasons. For one, the motors move in unison which is intuitive, if not pleasing, to observers. For another, there is only one command, steering angle, which need be considered an actuator in feedback control. The controller also commands the motors to turn in opposite directions (one in forward, the other in reverse). The physical meaning for the three actuators (steering angle, port thrust, and starboard thrust) within the control vector,  $\mathbf{u}_{prop}$ , are outlined in Table 9.

$$\dot{\mathbf{x}} = A_m \mathbf{x} + \mathbf{b} \left\{ \omega \begin{bmatrix} \cos \delta_1 (F_1 - F_2) \\ \sin \delta_1 (F_1 + F_2) \\ (B \sin \delta_1 - L \cos \delta_1) (F_1 + F_2) \end{bmatrix} (t) + (\boldsymbol{\theta})^T + \sigma(t) \right\} \quad (42)$$

**Table 9 Actuator Physical and Mathematical Models**

<b>u</b>	<b>Equation</b>	<b>Net Force/Moment</b>	<b>Motor RPM</b>	<b>Steering Angle</b>
<b>Surge</b>	$\cos \delta_1 (F_1 - F_2)$	Surge control forces are a function of: 1. Steering angle 2. Differential thrust	Different motor speeds will create differential thrust	Steering angle modulates the surge force (e.g., low angles maximize surge force for a given differential thrust)
<b>Sway</b>	$\sin \delta_1 (F_1 + F_2)$	Sway control forces are a function of: 1. Steering angle 2. Total thrust	Different motor speeds will create different levels of thrust; however, the sway force component is additive	Steering angle modulates the sway force (e.g., high angles maximize sway force for a given differential thrust)

<b>u</b>	<b>Equation</b>	<b>Net Force/Moment</b>	<b>Motor RPM</b>	<b>Steering Angle</b>
<b>Yaw</b>	$(B\sin\delta_1 - L\cos\delta_1)(F_1 + F_2)$	Yaw control moments are a function of: <ol style="list-style-type: none"> <li>1. The motor's moment arms</li> <li>2. Steering angle</li> <li>3. Total thrust</li> </ol>	Different motor speeds will create different levels of thrust; however, the two motors' thrust is additive to the net yaw control moment	Steering angle, relative to the moment arms, controls the sign and modulates the magnitude of the control moment. The moments are lowest near equilibrium point where $B\sin\delta_1 = L\cos\delta_1$ .

Given the physical meaning of the actuators in yaw, the control design allocated steering angle to yaw control. Assuming calm seas and no wind, to generate positive yaw, the controller must command a steering angle such that  $B\sin\delta_1 > L\cos\delta_1$ . For negative yaw,  $B\sin\delta_1 < L\cos\delta_1$ . Finally, for pure lateral translation the controller must command a steering angle such that  $B\sin\delta_1 = L\cos\delta_1$ . The magnitude of the moment is then dictated by the physical parameters of the boat and the sum of the two motors' thrust.

To control surge and sway, the control design takes advantage of the decoupled equations of motions and the fact that surge is controlled by differential thrust. The controller drives the surge velocity to zero by modulating the forward motor speed. At the same time, the controller commands the reverse motor speed to a calibrated speed. Although the controller could command reverse motor speed based on sway velocity feedback, it is assumed that there is an RPM range which is available for joystick maneuvers and that the calibrated reverse speed is proportional to the joystick deflection.

As such, the controller regulates surge speed through forward motor speed while it allows sway speed to be an open-loop resultant of the commanded steering angle, the forward motor speed, and the calibrated set point for the reverse motor speed:

$$\mathbf{u}_{prop} = \begin{bmatrix} u(\text{Differential Thrust}) \\ u(\text{Sway Calibration}) \\ u(\text{Steering Angle}) \end{bmatrix} \quad (43)$$

$$= \begin{bmatrix} \cos \delta_1 k \{(RPM_2 + \Delta) - RPM_2\} \\ \sin \delta_1 k \{(RPM_2 + \Delta) + RPM_2\} \\ (B \sin \delta_1 - L \cos \delta_1) k \{(RPM_2 + \Delta) + RPM_2\} \end{bmatrix} \quad (44)$$

$$= \begin{bmatrix} \cos \delta_1 k \Delta \\ \sin \delta_1 k (\Delta + 2RPM_2) \\ (B \sin \delta_1 - L \cos \delta_1) k (\Delta + 2RPM_2) \end{bmatrix} \quad (45)$$

Where

$k = \text{unknown propeller gain}$   
 $\Delta = \text{differential RPM}$

However, to make the commanded input,  $u_{thr}$ , simply

$$u_{thr} = \begin{bmatrix} \Delta \\ \text{open loop} \\ \delta_1 \end{bmatrix} \quad (46)$$

the controller needed a transfer function from net surge thrust to differential thrust and from net control torque to steering angle.

Once the control allocation decisions were made, the next step was to leverage the adaptive parameters in the LIAC to solve the crux of the problem. Unlike most DP and autopilot controllers, the neutral position for yaw control is not known. The steering angles which apply positive, zero, or negative torque are unknown because the distance



to the COLR is unknown. To overcome this obstacle, a new approach to adapting to the unknown actuator gain was needed.

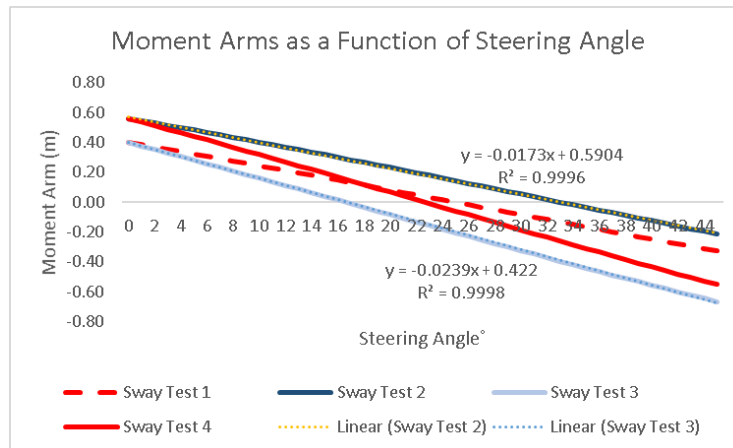


**Figure 8 Moment Arms as a Function of Steering Angle**

The insight which led to the final approach was created by thinking of the mathematical model and the L1 Adaptive Control architecture together. Reflecting on the mathematical model, the moment arm created by the range of steering angles (and therefore, the control moment) is a nearly linear function of steering angle. Figure 8 illustrates this relationship for the four test scenarios. The dependent variable on the y-axis is the moment arm length for the test boat in each scenario. For each scenario, there are two adjustable boat parameters which change the amount of torque the motors' thrust can apply to the floating boat. The first being the distance from the motors to the boat centerline – narrow spacing and wide spacing. The second being the location of the COLR - forward COLR and aft COLR. Therefore, the distance from the motors to the pivot point varies with each scenario. The independent variable on the x-axis is the steering angle. At  $0^\circ$ , the motors are pointing straight forward, while at  $45^\circ$ , the motors are pointed inward all the way to their physical limit. As the motors turn inward, the moment applied decreases, reaches zero when the motors are pointed at the COLR, and

then increases in the opposite direction until the steering mechanism hits the stop. The difference in moment arm from one test scenario to another can be described as changes in slope and y-intercept. Meanwhile, the Adaptive Law adapts for unknown actuator gain,  $\omega_3$ , and unknown disturbance moments,  $\sigma_3$ , separately. Mathematically, the unknown actuator gain is like the slope and the adaptive disturbance variable could be considered a combination of the y intercept adjustment and disturbances. From these observations, a fixed factor was added to the state estimator for the lowest y intercept such that the difference between the baseline assumption and the actual geometry could be resolved by estimating  $\omega_3$  up from a minimum of 1 to the maximum  $\omega_3$ . Likewise,  $\sigma_3$  limits were set to adapt the y intercept adjustment as well as disturbances.

Lastly, the controller's two low pass filters were designed through trial and error to separate the high frequency system identification signal from the actuators. The final design was a second order low-pass yaw filter for surge and sway/yaw subsystems.

At the end of the control design phase, a reference system, control allocation strategy, and strategy for adapting to an unknown neutral yaw moment steering position were created. The physical and mathematical model were used to develop insights around which judgment could be applied to implement an L1 Adaptive Control architecture in MATLAB. There, the design decisions were tested and refined in iterative simulation testing.

## IV. SIMULATION RESULTS

Before implementing the controller in the test boat, the controller was simulated in MATLAB as a way of predicting test boat performance for refining the controller design. Naturally, the controller design required definition of the L1AC modules. The design also required engineering judgment to create a solution to the crux of the sway control challenge – unknown actuator magnitude and neutral position. By combining engineering judgment and creativity, the controller design was refined iteratively in MATLAB before arriving at the design chosen for hardware implementation and test.

For the iterations to be meaningful, the controller design required a proper L1AC architecture on which to build. An L1AC generic architecture was created in MATLAB. The projection operator code is provided in Appendix D. The MATLAB code was verified by comparing the code's output with Hovakimyan (2010). The reference problem simulated a linear system under a few input scenarios to test the scalability of the adaptive control. The generic controller recreated the published results which proved the state predictor, reference model, and control filters were ready to be modified for the test boat.

After the L1AC baseline code was validated, the joystick controller was implemented and used to simulate four variant boat models in a pure translation maneuver (sway). The four simulations were designed to simulate the scenarios which were used in the physical tests. As shown in Tables 10-14 and Figures 9-18, the four models varied the plant matrix values which simulated different inertial properties and

motor configurations. Wind disturbances were also simulated. The simulations demonstrate the controller's performance.

The simulated boat motion was compared to the ideal to test the controller's acceptability. In all cases, the yaw rate oscillated around zero radians per second. The sway velocity also oscillated while increasing overall. As expected, while the adaptive parameters oscillated, the steering command also varied but at a much lower rate. In the case of wind disturbance, the controller detected the wind and adapted properly. Overall, the simulated LIAC controller performed well across all scenarios in sway-yaw coupled motion.

**Table 10 Light Weight Narrow Motors Plant Parameters**

Plant Parameter	Value
Plant Model Matrix	$A_p = \begin{bmatrix} -0.003884 & 0.002266 \\ -0.001476 & -0.001107 \end{bmatrix}$
Length at Waterline	1.2 m
Draft Below Waterline	0.06 m
Motor to Centerline Distance	0.19 m
Motor to Center of Lateral Resistance Distance	0.60 m
Disturbance	None

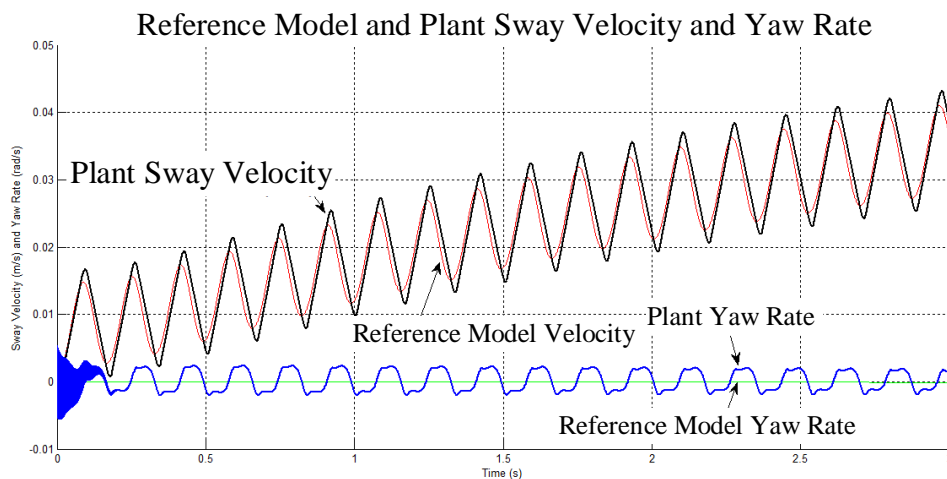


**Figure 9 Light Weight Narrow Motors Simulation**

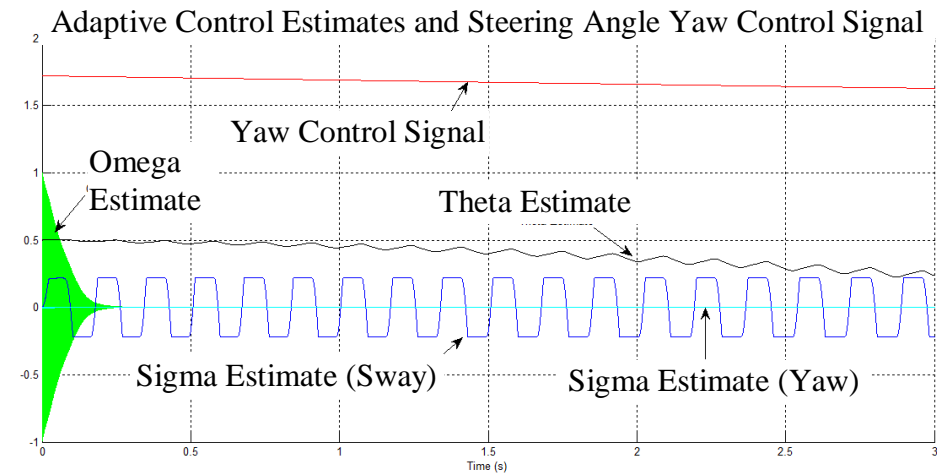


**Figure 10 Light Weight Narrow Motors Simulation Parameter Estimates**

**Table 11 Light Weight Wide Motors Plant Parameters**

Plant Parameter	Value
Plant Model Matrix	$A_p = \begin{bmatrix} -0.003884 & 0.002266 \\ -0.001476 & -0.001107 \end{bmatrix}$
Length at Waterline	1.2 m
Draft Below Waterline	0.06 m
Motor to Centerline Distance	0.28 m
Motor to Center of Lateral Resistance Distance	0.60 m
Disturbance	None

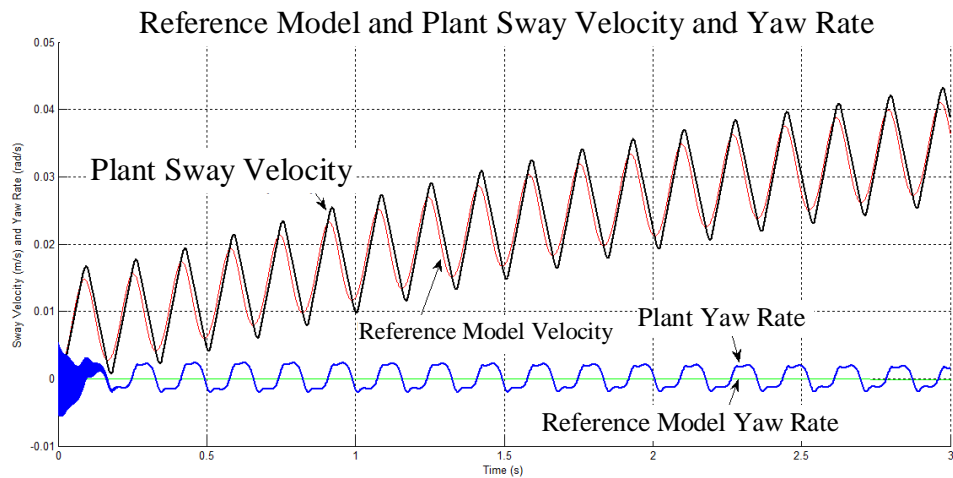


**Figure 11 Light Weight Wide Motors Simulation**

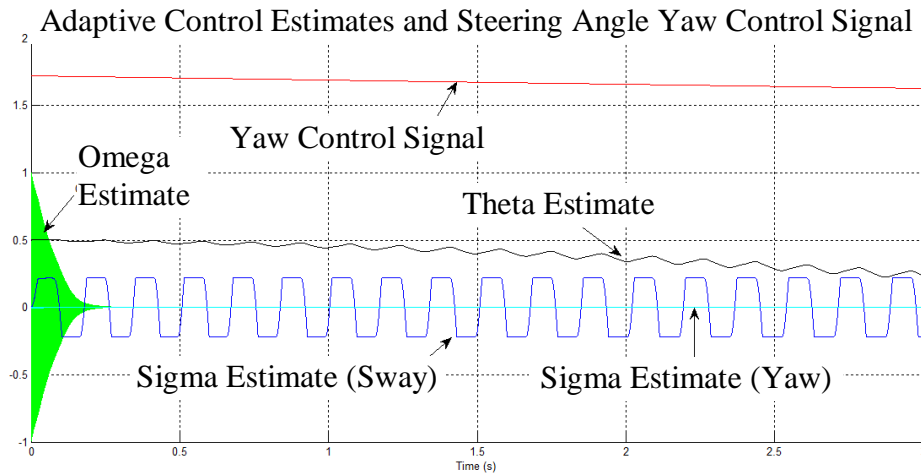


**Figure 12 Light Weight Wide Motors Simulation Parameter Estimates**

**Table 12 Light Weight Wide Motors Parameters**

Plant Parameter	Value
Plant Model Matrix	$A_p = \begin{bmatrix} -0.003884 & 0.002266 \\ -0.001476 & -0.001107 \end{bmatrix}$
Length at Waterline	1.2 m
Draft Below Waterline	0.06 m
Motor to Centerline Distance	0.28 m
Motor to Center of Lateral Resistance Distance	0.60 m
Disturbance	0.2 N sway, 0.2 Nm yaw

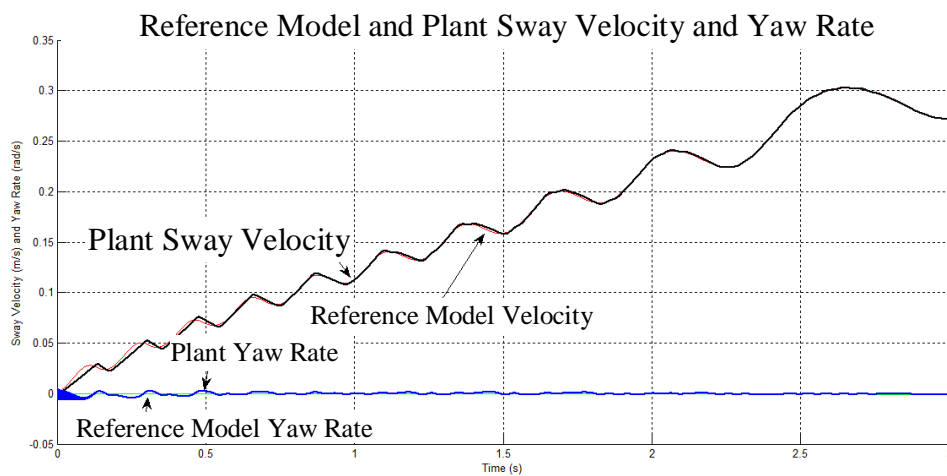


**Figure 13 Light Weight Wide Motors Simulation with Wind Disturbance**

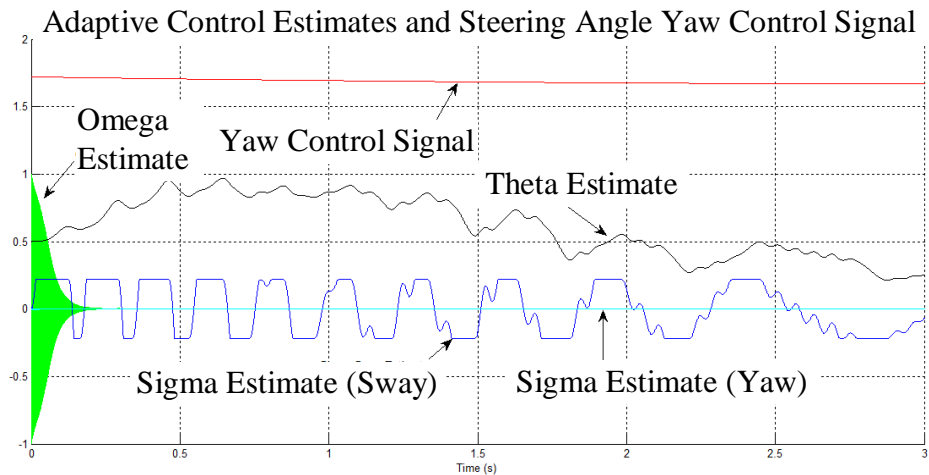


**Figure 14** Light Weight Wide Simulation Parameter Estimates with Wind Disturbance

**Table 13** Heavy Weight Narrow Motors Parameters

Plant Parameter	Value
Plant Model Matrix	$A_p = \begin{bmatrix} -0.003501 & 0.001915 \\ -0.001247 & -0.000599 \end{bmatrix}$
Length at Waterline	1.25 m
Draft Below Waterline	0.065 m
Motor to Centerline Distance	0.19 m
Motor to Center of Lateral Resistance Distance	0.64 m
Disturbance	None

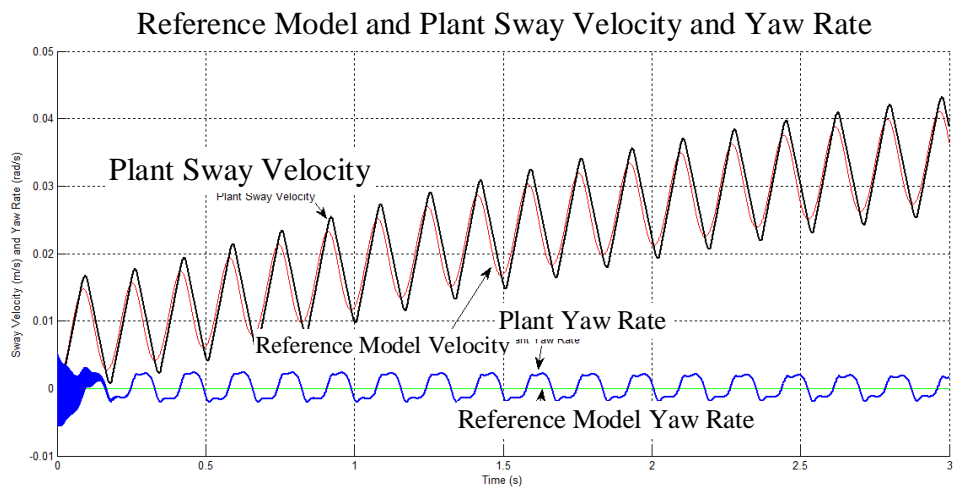


**Figure 15 Heavy Weight Narrow Motors Simulation**

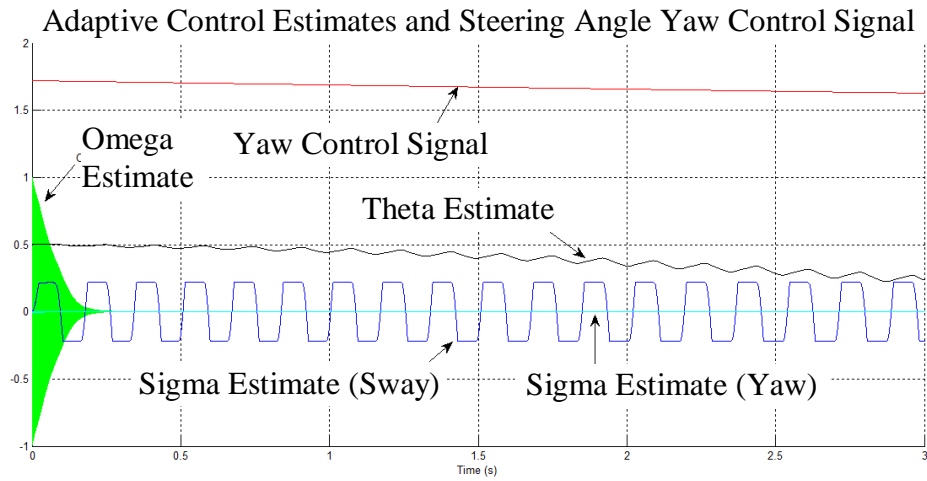


**Figure 16 Heavy Weight Narrow Motors Simulation Parameter Estimates**

**Table 14 Heavy Weight Wide Motors Parameters**

Plant Parameter	Value
Plant Model Matrix	$A_p = \begin{bmatrix} -0.003501 & 0.001915 \\ -0.001247 & -0.000599 \end{bmatrix}$
Length at Waterline	1.25 m
Draft Below Waterline	0.065 m
Motor to Centerline Distance	0.28 m
Motor to Center of Lateral Resistance Distance	0.64 m
Disturbance	None



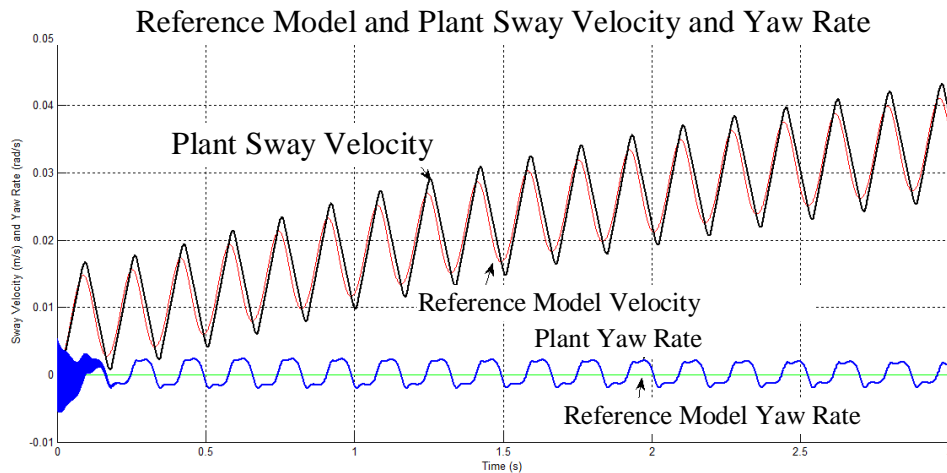


**Figure 17 Heavy Weight Wide Motors Simulation**

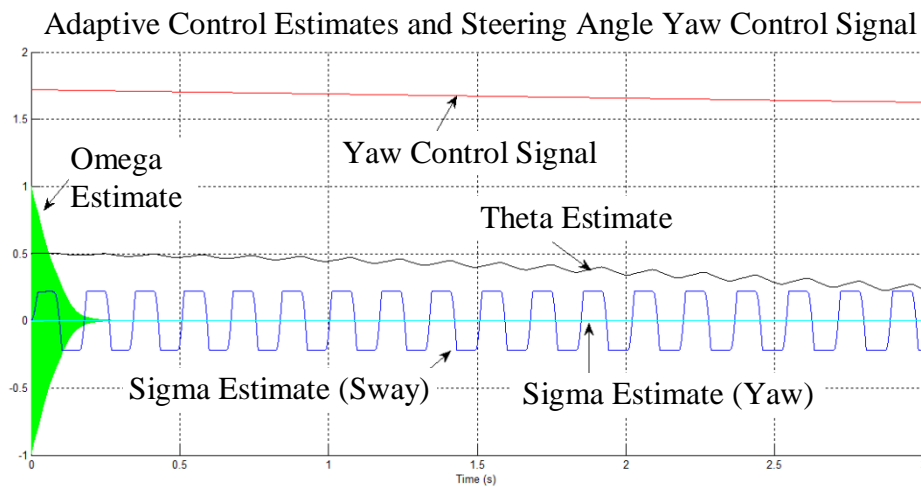


**Figure 18 Heavy Weight Wide Motors Simulation Parameter Estimates**

Analysis of the simulations provided invaluable information regarding the controller design. For each simulated scenario, yaw rate and sway velocity was compared to the reference model as shown in Figures 9-18. The simulations predicted close tracking between the reference boat and the test boat in sway velocity and in yaw rate. The simulations also predicted low-amplitude oscillations in yaw rate. Yet, the oscillations in the yaw control signal were low in magnitude when compared to the oscillations in the adaptive estimates. The promising simulated performance in tracking

and adaption without oscillations in the control signal align with the main features of L1 Adaptive Control.

The critical finding in the analysis was that two aspects of the control affect the ability to adapt. For one, the engines must produce the right amount of torque. If the generated moment is too small, then the boat will rotate as it sways for the lack of a sufficient moment to balance the hydrodynamic forces. If the moment is too large, then the adaptive controller over-controls the boat which essentially creates controller-induced oscillations. Together, the above analysis proved that the control allocation strategy and L1AC controller design combined to be a promising solution.

## V. TEST RESULTS

After seeing promising results in simulation, the controller was implemented in the test boat for yaw control and stationary rotation testing. The test data was collected in a scaled, controlled test environment designed to predict full scale dynamic behavior. As described more below, the test boat was built to scale to have dynamics like the target application. The practice of using scale models as a means for obtaining experimental data was initiated by Froude that a model boat's resistance will be the same as the full-scale boat if they have the same Froude number (Lewis, 1988). Similarly, the test tank was designed to meet specific dimensional requirements for scale testing. To create disturbance forces, an electric fan provided a consistent wind effect. Finally, motion capture technology collected the test boat's dynamic behavior. Together, the test boat, tank, fan, and measurement tools created an adequate system to build on theoretical modeling with real world, albeit scaled, data.

### A. Test Equipment

As a critical part of the test protocol, the test boat was designed to achieve several research goals. In alignment with the model based systems engineering approach, the mathematical model needed to closely match the test boat. Given the complex three-dimensional geometry, the best method for creating the inertia matrix estimates was to leverage CAD calculations. Hence, the boat was designed in CAD which also allowed the test boat geometry to resemble the target applications. The design also had to provide a way to vary specific boat parameters to replicate the variations between boat models and boat brands. Once designed, the test boat was built from balsa wood with a full keel

and plank on frame construction. As such, the test boat was the realization of the CAD model and suitable for mathematical modeling and testing.

The test boat architecture matched that of the target application (i.e., large center console fishing boat or cruiser) in three important ways. First, the boat was designed and built to have similar hydrodynamic properties as its full-scale counterpart. The resistance from waves is assumed to be the same for a model and a full-scale boat at the same Froude number. Froude first observed that scale models predict full scale behavior (Lewis, 54). Froude contended that a boat's total resistance is the sum of the direct resistance due to waves and the resistance from friction so he used a dimensionless quantity calculated according to the equation in the Table 15 below to show when a scale model would perform similarly to the full-size boat. Table 15 outlines the equivalent Froude number for the test boat's actual sway speed as well as two typical target applications assumed to perform the translation maneuver at about 0.5 mile per hour or 0.2 meters per second.

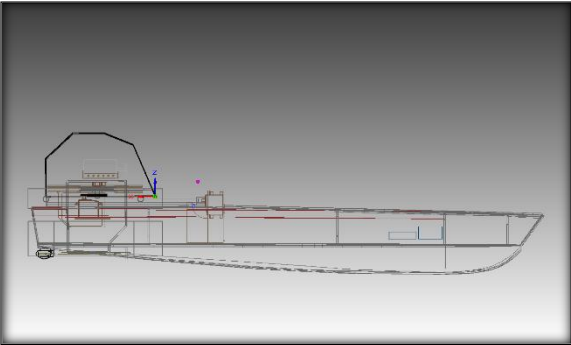


**Table 15 Test Boat and Target Application Froude Numbers**

<b>Froude Number</b>		<b>Test Boat</b>	<b>320 Outrage</b>	<b>370 Sundancer</b>
$F_n = \frac{\text{speed (m/s)}}{\sqrt{\text{gravity (m/s}^2) * \text{length at waterline(m)}}}$	<b>Target Speed</b>	0.07 m/s	0.2 m/s	0.2 m/s
	<b>Length</b>	1.2	9.8	11.4
	$F_n$	0.2	0.2	0.2

The resistance due to hydrodynamic friction was assumed to be negligible at low speeds. Second, the test boat's hull shape mimics the full-scale boat to recreate the pressure field created by hydrodynamic forces. The pressure field is critical to the test because the point around which the boat will rotate can be thought of as the resultant force of

integrating the pressure field over the length of the boat. Hence, the deadrise and keel shape were built to follow the form of the target applications. Tables 16 and 17 show the similarities in profile shape between the test boat and two target applications (Lemancik, 2009). By making the hull shape the same as the full-scale boat's shape, the center of lateral resistance is in a similar location.

**Table 16 Test Boat and Target Application Images**

Vessel	Image
Test Boat	
320 Outrage	
370 Sundancer	

**Table 17 Test Boat and Target Application Characteristics**

	<b>Test Boat</b>	<b>320 Outrage</b>	<b>370 Sundancer</b>
<b>Length (L)</b>	1.2m	9.8 m	11.4 m
<b>Beam (B)</b>	0.3m	3.1 m	3.7 m
<b>L/B Ratio</b>	4	3.2	3.1
<b>Deadrise</b>	25°	23°	21°
<b>Motors</b>	2	2-4	2
<b>Propulsion</b>	DC Motor	Outboard	Sterndrive

Third, the test boat was designed with features for varying critical parameters. The outboard motors could slide in and out to test the controller's ability to adapt when the relationship between the engines and the boat geometry is not known. Also, the boat was built with ballast compartments to move the center of gravity forward and aft as needed. Moving the center of gravity changed the boat's stance which changed the shape of the pressure field which ultimately changed the center of lateral resistance. The net result was one test boat which both resembled the target applications and offered a means to vary its geometry to recreate the variety of full scale recreational boats and their dynamics.

The test tank and fan provided a stable, consistent environment for each test scenario. For the most part, the tank provided enough maneuvering space to justify assumptions made in the mathematic model. To be considered open water, the hull must be at least three beam widths from boundaries; otherwise, the hydrodynamic forces can change significantly during maneuvers (Lewis, 279). In restricted water, the boundaries will alter the hydrodynamic forces by introducing flow effects whenever the hull centerline is closer to one boundary, port or starboard, than the other (Lewis, 285).

Figure 19 is a scaled representation of the test tank boundaries and the test boat. The concentric circles centered on the boat outline the maneuvering room in increments of

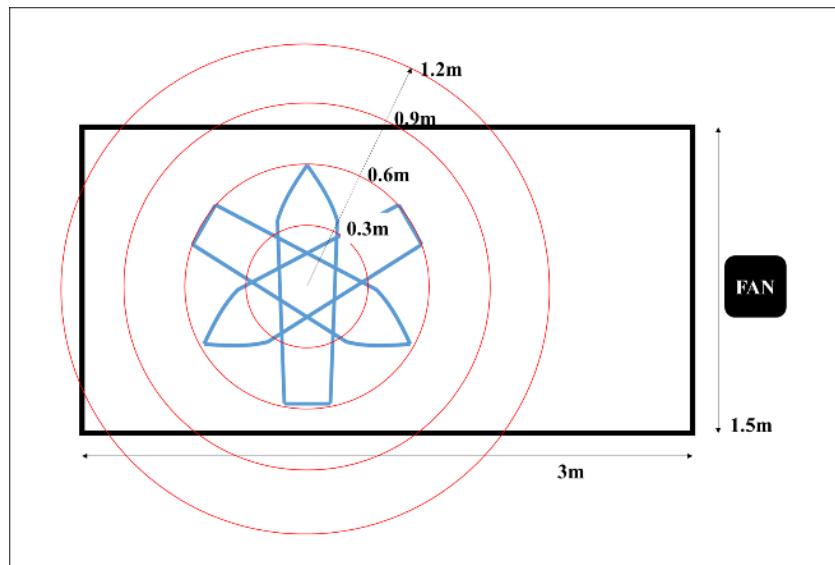


**Figure 19 Test Tank**

one beam width. From observation, the tank walls likely created some minor flow effects during portions of each rotation. As in the x and y axis, there are guidelines for depth in the z axis. To be considered deep, the water must be three times the hull's draft; otherwise, the hull will experience changes in turning diameter proportional to the ratio of the draft to water depth (Lewis, 279). The water depth was measured before the test to ensure proper performance. The tank itself was constructed with a PVC pipe frame covered with layers of plastic sheets. To test the controller's ability to adapt to disturbances, a test fan provided a repeatable wind disturbance. Lastly, the camera was mounted above the tank within reach for recording. The full system provided an adequate testing environment.

## B. Test Method

Given a stable environment, the measurement system generated data to analyze the test boat dynamics under LIAC control. The measurement system consisted of a digital camera, motion capture software, and a laptop computer. The camera was

positioned approximately six feet above the surface of the water. From there, the camera captured video of each test run in a digital movie file. The movie file was uploaded to motion capture software. To track the test boat's motion, the software tracks designated points on the test boat.

Within the motion capture data collection process, there are two sources of minor error. First, the scale is provided manually to the software; therefore, there may be scaling error of less than 5mm. Second, there is some error in the motion tracking itself because the tracking designation is placed manually which means that each designation is within an approximate 5mm radius of the precise point to be tracked. While the manual designation process does introduce some measurement error, the error can be removed through smoothing. With a test boat length of approximately one meter and a lateral translation distance of about one meter, the measuring system would have need to be accurate within 0.1 meters or ten percent. Considering the precision needed to assess the controller's performance, the measurement system captured useful data by obtaining accuracy within one 0.01 meters or one percent of the boat length.

### C. Test Cases

The test scenarios performed at the limits of adaptability and control for lateral translation and stationary rotation. For the lateral translation maneuver, the engines are positioned at two different distances from the test boat's centerline and the boat loadout was varied between light and heavy weights to create a total of four individual tests. These four variations simulate the variation in beam widths and in boat lengths which can be found in the market. For the test boat, the narrow and wide position test the controller



at the physical limits of the test boat. If the motors were any closer in the narrow test or farther away in the wide test, the motor swivel mechanisms would collide with the hull or outrigger respectively. The light weight test is the empty weight of the test boat. The boat was designed such that the COLR, when empty, would be approximately 0.4 meters from the bow or about 33% of the boat length. During testing, several ballasts were considered; however, the ballast used for the heavy test was selected because it moved the COLR forward approximately 0.06 meters. This distance was enough to be noticeable and pushed the controller to the limit in the narrow motor, heavy load test. Table 18 outlines the settings for each scenario.

**Table 18 Sway Test Scenarios**

<b>Test Scenario</b>	<b>Engine to Centerline Distance</b>	<b>Load</b>	<b>Wind Disturbance</b>
Sway Test 1	Narrow	Light	No
Sway Test 2	Wide	Light	No
Sway Test 3	Narrow	Heavy	No
Sway Test 4	Wide	Heavy	No

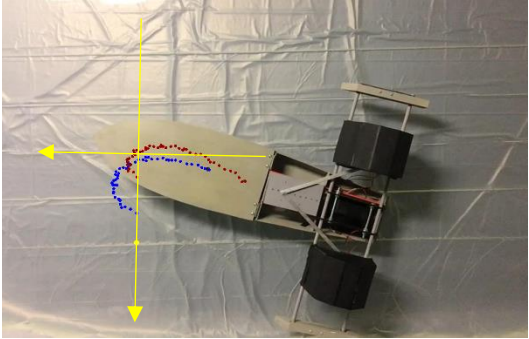
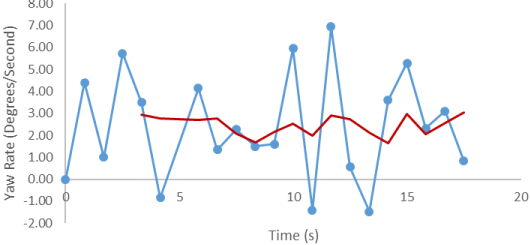
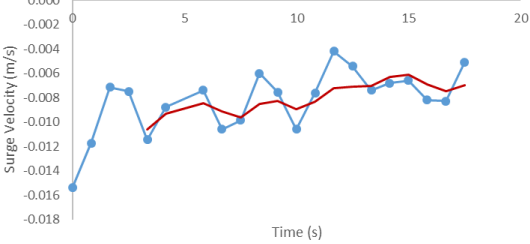
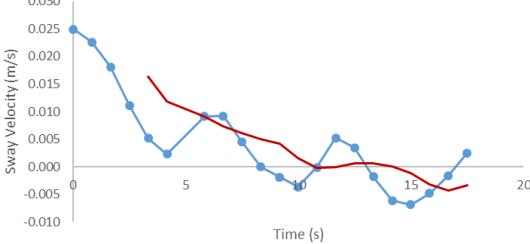
For the stationary rotation maneuver, the motors were positioned at a consistent distance from centerline while the loadout was varied to create two scenarios. In the yaw test, positioning the motors at different distances would not present the controller with a materially different problem because the steering angles are so low. Wider motor-to-centerline distances would only increase the yaw rate for the same motor speed. The two scenarios were repeated with a wind disturbance to create scenarios three and four as outlined in Table 19.

**Table 19 Yaw Test Scenarios**

<b>Test Scenario</b>	<b>Engine to Centerline Distance</b>	<b>Load</b>	<b>Wind Disturbance</b>
Yaw Test 1	Narrow	Light	No
Yaw Test 2	Narrow	Light	Yes
Yaw Test 3	Narrow	Heavy	No
Yaw Test 4	Narrow	Heavy	Yes

Table 20 shows the impact the wind disturbance had on the boat while dead in the water. The first column is a picture of the actual test. In the picture, the blue and red dotted lines trace the path of the tracking points on the boat. The yellow lines mark the inertial axis. The second column has three charts which plot yaw rate, surge velocity, and sway velocity respectively. A ten-point averaging trend line has been added to filter noise in the data. In the wind, the boat turned bow into the wind and was pushed back at approximately 0.01 meters per second which is about 20% of the test sway velocity.

Table 20 Wind Disturbance Effects

Motion Capture	Velocities
	<p data-bbox="971 289 1198 331">Light Weight, Wind, No Power Yaw Rate (Degrees/Second)</p> 
	<p data-bbox="971 630 1198 672">Light Weight, Wind, No Power Surge Velocity (m/s)</p> 
	<p data-bbox="971 966 1198 1008">Light Weight, Wind, No Power Sway Velocity (m/s)</p> 

#### D. Test Procedure

For the all tests, the boat began at rest with zero rudder angle, zero motor rpm, and the controller turned off. After a delay, the controller engaged with a constant command input as described in Table 21.

**Table 21 Commanded Inputs**

<b>Test Maneuver</b>	<b>Commanded Yaw Rate</b>	<b>Commanded Sway Speed</b>	<b>Commanded Surge Speed</b>
Sway Test (1 through 4)	$0 \frac{deg}{s}$	$0.07 \frac{m}{s}$	$0 \frac{m}{s}$
Yaw Test (1 through 4)	$8 \frac{deg}{s}$	$0 \frac{m}{s}$	$0 \frac{m}{s}$

#### E. Test Data

The test data was collected and processed to analyze the controller's performance in each test scenario. To create the data, the motion capture software, *Video Physics*, was advanced in 0.17 second increments (5 frames) for the duration of the maneuver. At each increment, the software tracked two specific points on the boat hull. One point was the blue LED light and the other was the push button switch. Both points lie on the boat's centerline. Once created, the data was exported to Excel for further processing. The raw position and velocity data was smoothed through averaging and Cartesian coordinates were converted to yaw angles. Next, the data was plotted on charts for better visualization. Finally, the error between ideal and actual position and velocity was calculated. As such, the raw data was used to analyze the controller's performance.

The tables below depict how the controller performed in each sway test. Table 22 also outlines the error for each scenario and the heading change after moving three beam widths to starboard. Table 24 outlines the yaw rate test results for each sway test scenario. The first column identifies the test number.

For the sway tests, the motion capture software provided estimates for position and velocity in surge and sway directions. The software tracked two points (traced in

blue and red in the pictures within Table 24). After capturing the test boat coordinates in the motion capture software, the coordinates were exported to Excel for estimating motion error to be used for analysis. To estimate the yaw rate error, first the yaw angle was estimated from the changes in the coordinates of the two points:

$$\psi = \tan^{-1} \left[ \frac{(y_1 - y_2)}{(x_1 - x_2)} \right]$$

The average yaw rate between motion capture points was calculated by dividing the change in yaw angle by the change in time. Before calculating the yaw rate error, the manual designation error was minimized by calculating a ten-point moving average over each test. Finally, to calculate the yaw rate error, the smoothed yaw rate for each 0.17 second interval was subtracted from the target, 0 radians/second. To estimate the surge error, the motion capture software estimates for surge velocity were used directly. However, to smooth the designation error, a ten-point moving average was used as described above. Once the error was estimated for each maneuver, the data was used to calculate several norms as outlined in Table 22. Additionally, the yaw angle at three beam widths was calculated to compare the system performance to the design target. Combined, the error calculations quantify the controller's performance under all scenarios.

**Table 22 Sway Test Error Calculations**

<b>Sway Maneuver Yaw Rate Error</b>	<b>Error Calculation</b>	<b>Sway Test 1</b>	<b>Sway Test 2</b>	<b>Sway Test 3</b>	<b>Sway Test 4</b>
Infinity norm	$maximum\ error_{i=1}^n$	$2.8\frac{deg}{s}$	$2.5\frac{deg}{s}$	$2.9\frac{deg}{s}$	$3.6\frac{deg}{s}$
2-norm	$\sqrt{\frac{\sum_{i=1}^n (error_i)^2}{n}}$	$8.1\frac{deg}{s}$	$6.2\frac{deg}{s}$	$7.1\frac{deg}{s}$	$10.0\frac{deg}{s}$
1-norm	$\sum_{i=1}^n \ error\ $	$42.8\frac{deg}{s}$	$32.7\frac{deg}{s}$	$38.9\frac{deg}{s}$	$54.1\frac{deg}{s}$
Heading Change at 0.9m	$\tan^{-1} \left[ \frac{(y_1 - y_2)}{(x_1 - x_2)} \right]$	12.2°	10.7°	8.7°	16.0°

Like the yaw test results above, the tables below depict how the controller performed in each sway test. Table 23 outlines the yaw test results for each rotation scenario. The first column identifies the test number. The second column is a picture of the actual test. In the picture, the blue dotted lines trace the path of the tracking points on the boat during one full rotation. Only Yaw Test 3 made two rotations. The second rotation is traced in red. The third column is a plot of the ideal and actual position against time. Finally, Table 23 outlines the error for each scenario and distance the tracking point moved during a single rotation. Table 23 also shows the same data but for the second rotation in Yaw Test 3.

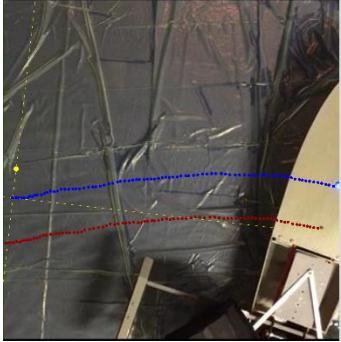
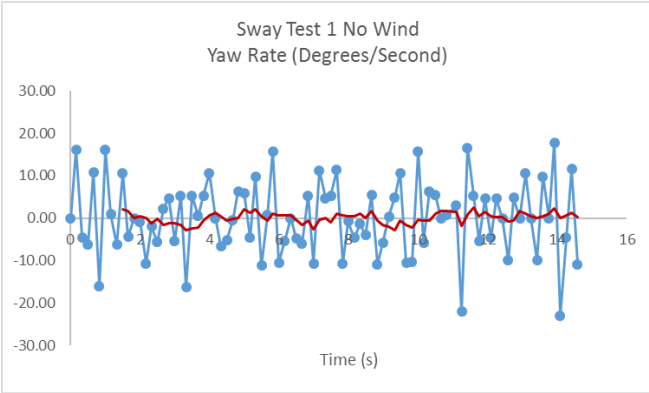
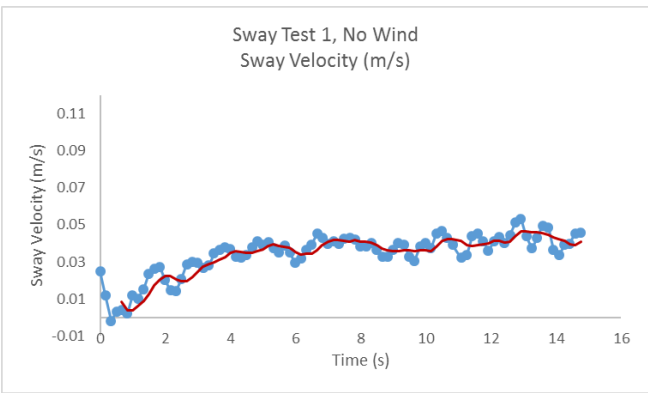
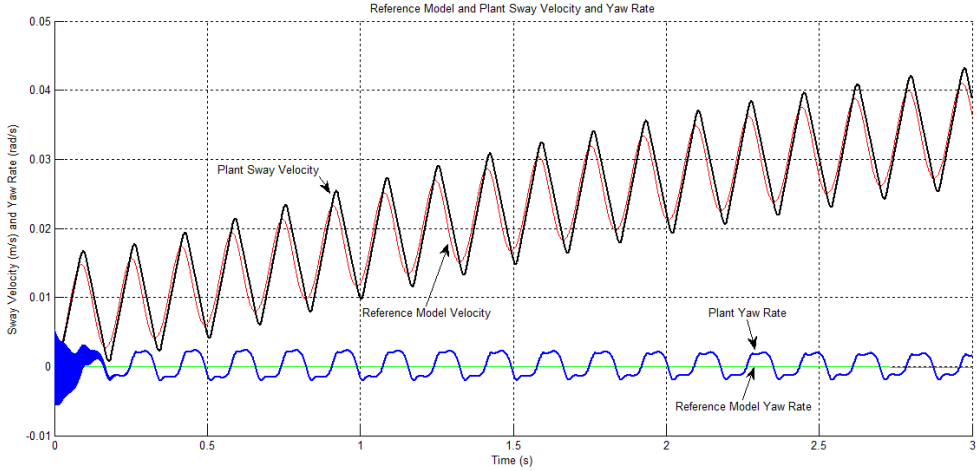
As in the sway tests, after capturing the test boat coordinates in the motion capture software the coordinates were exported to Excel for analysis. However, for the rotation tests the error was calculated by subtracting actual position of the designated point from the ideal position. A detailed description is included in the Appendix.

**Table 23 Yaw Test Error Calculations**

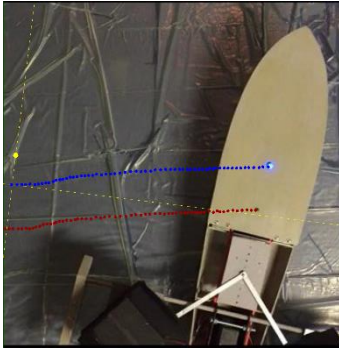
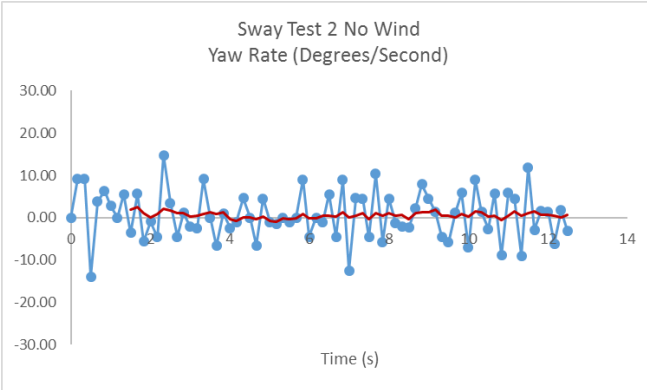
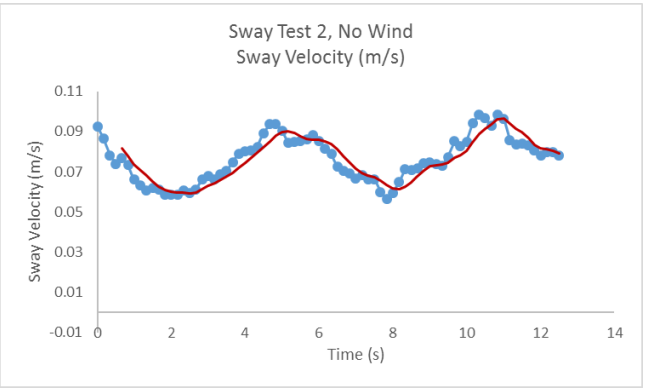
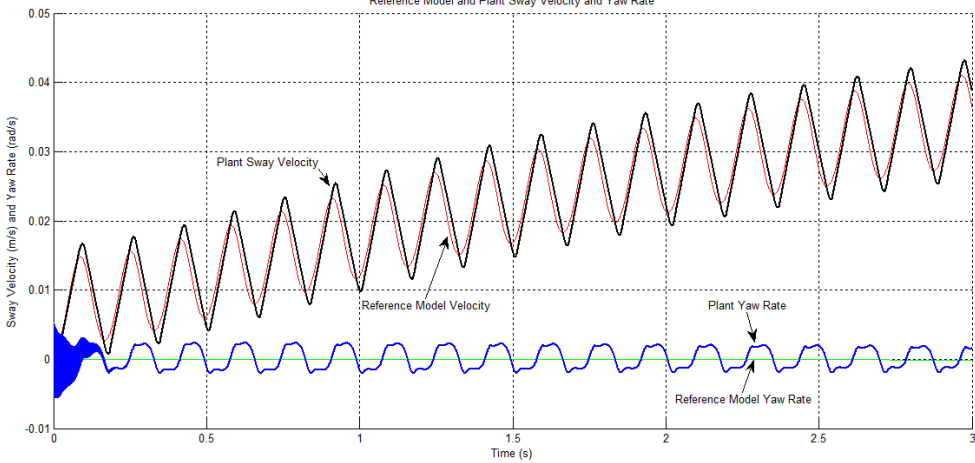
<b>Yaw Maneuver Position Error, 1st Rotation</b>	<b>Error Calculation</b>	<b>Yaw Test 1</b>	<b>Yaw Test 2</b>	<b>Yaw Test 3</b>	<b>Yaw Test 4</b>
Infinity norm	$maximum\ error_{i=1}^n$	0.07 m	0.13 m	0.07 m	0.20 m
2-norm	$\sqrt{\frac{\sum_{i=1}^n (error_i)^2}{n}}$	0.05 m	0.09m	0.03 m	0.33 m
1-norm	$\sum_{i=1}^n \ error\ $	3.39 m	5.91 m	4.49 m	7.68 m
Distance Moved After 1 Rotation  (% of boat length)	$\sqrt{(x^2 + y^2)}$	0.06 m (5%)	0.09 m (8%)	0.02 m (2%)	0.14 m (12%)

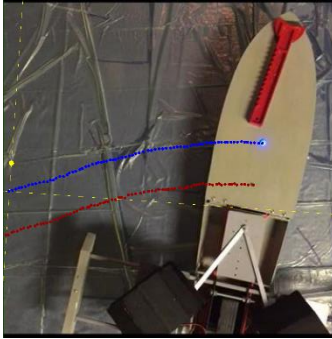
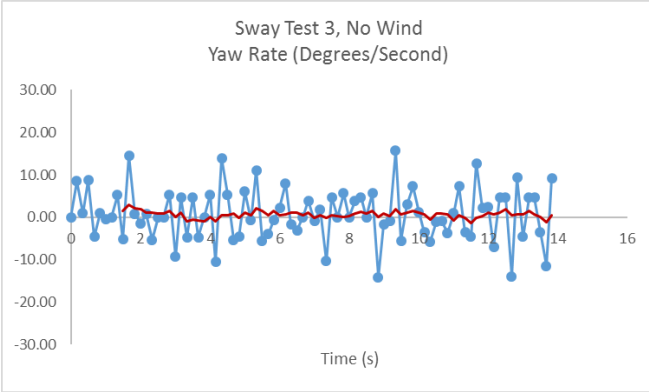
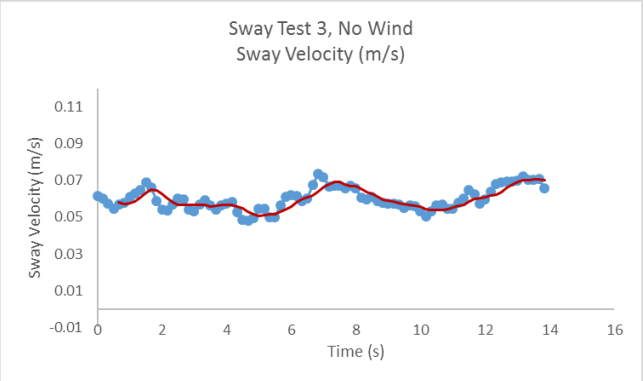
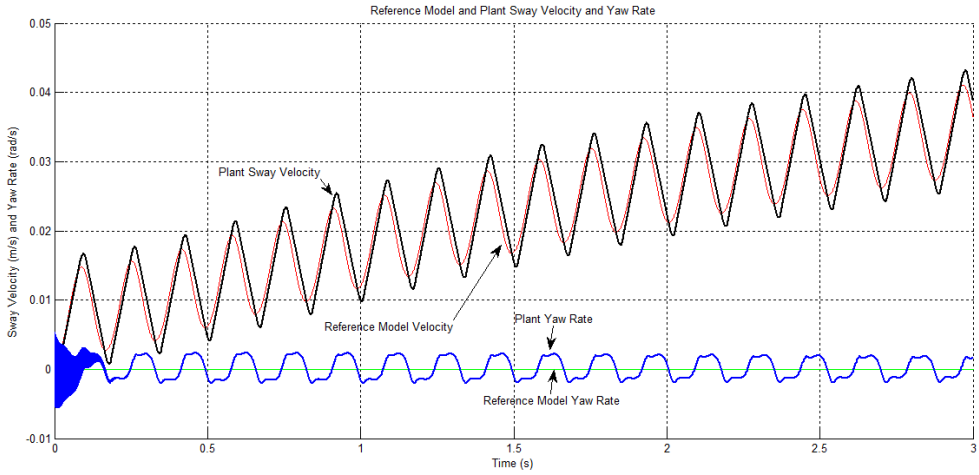
<b>Yaw Maneuver Position Error, 2nd Rotation</b>	<b>Error Calculation</b>		<b>Yaw Test 2</b>	
Infinity norm	$maximum\ error_{i=1}^n$		0.11 m	
2-norm	$\sqrt{\frac{\sum_{i=1}^n (error_i)^2}{n}}$		0.09 m	
1-norm	$\sum_{i=1}^n \ error\ $		6.14 m	
Distance Moved During 2nd Rotation  (% of boat length)	$\sqrt{(x^2 + y^2)}$		0.0 m (0%)	

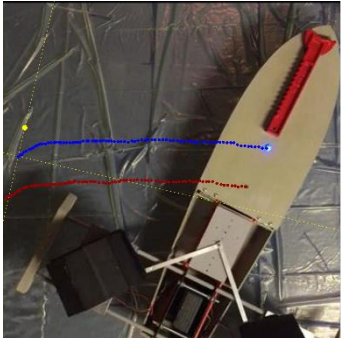
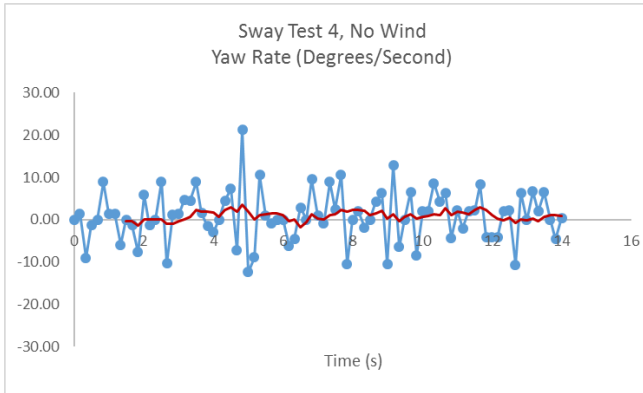
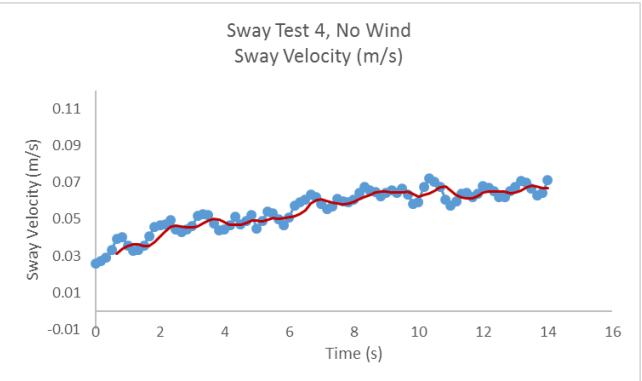
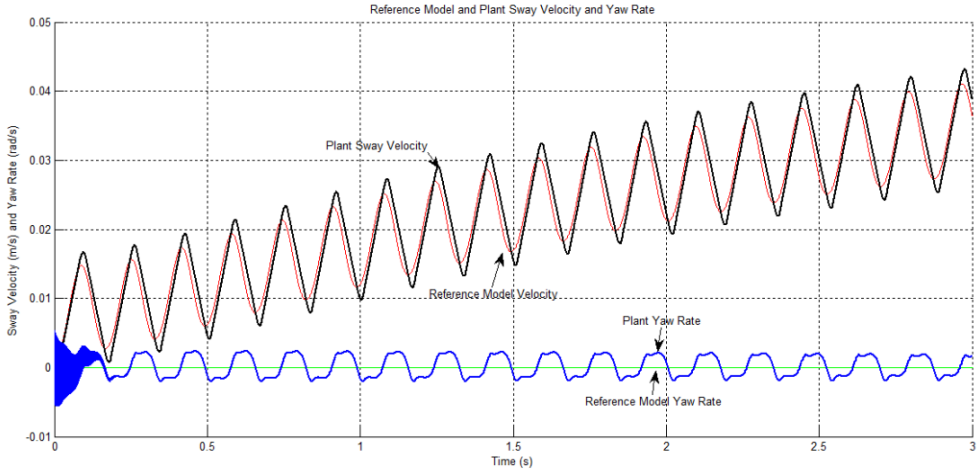
**Table 24 Sway Test Data**

Sway Test	Motion Capture	Yaw Rate	Sway Rate
1			
	<p>MATLAB Simulation of the Light Weight Narrow Motor Scenario</p>		

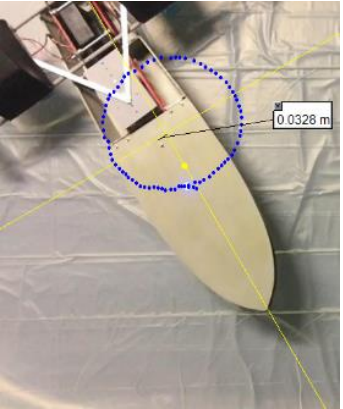
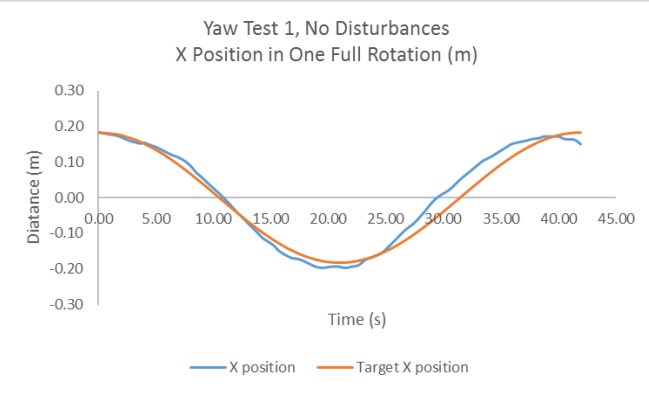
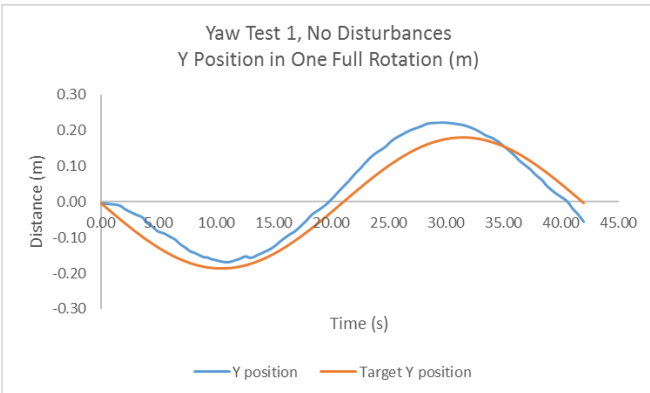
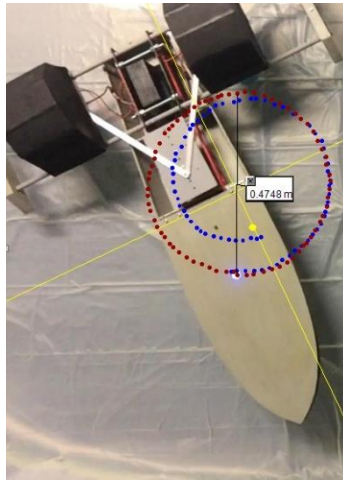
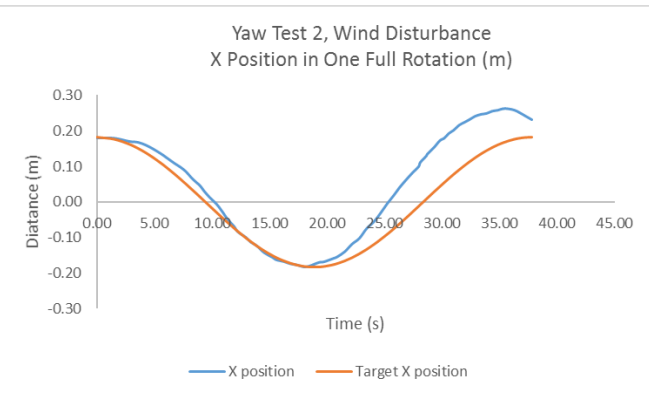
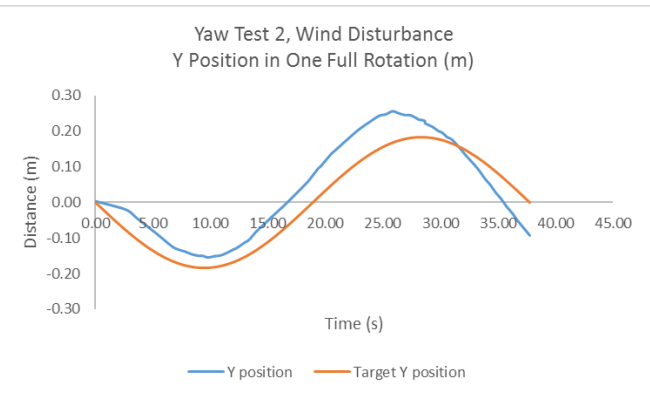


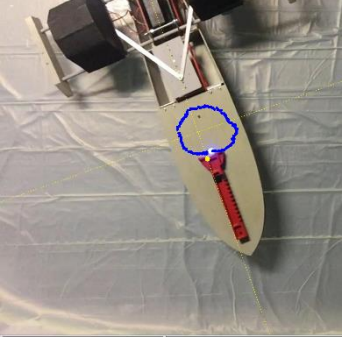
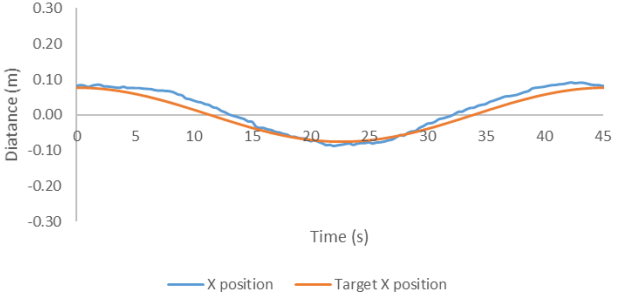
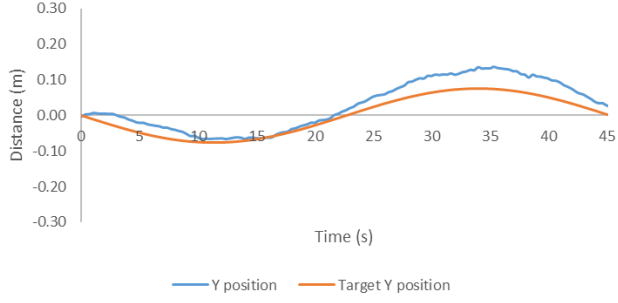
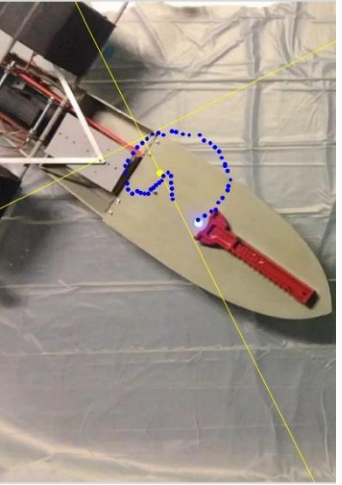
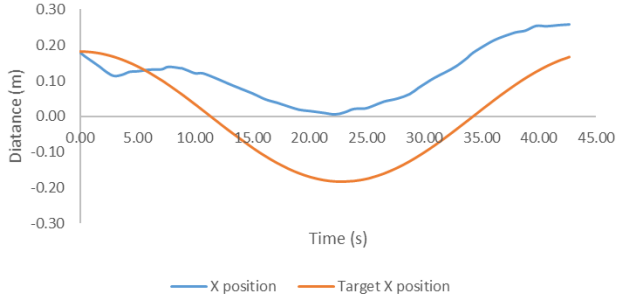
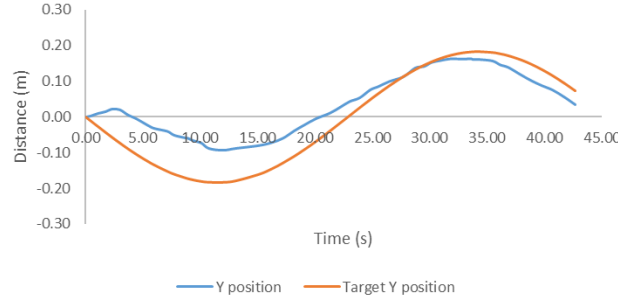
Sway Test	Motion Capture	Yaw Rate	Sway Rate
		<p style="text-align: center;">Sway Test 2 No Wind Yaw Rate (Degrees/Second)</p> 	<p style="text-align: center;">Sway Test 2, No Wind Sway Velocity (m/s)</p> 
<p style="text-align: center;">2</p>	<p style="text-align: center;">MATLAB Simulation of the Light Weight Wide Motor Scenario</p>	<p style="text-align: center;">Reference Model and Plant Sway Velocity and Yaw Rate</p> 	

Sway Test	Motion Capture	Yaw Rate	Sway Rate
3		<p>Sway Test 3, No Wind Yaw Rate (Degrees/Second)</p> 	<p>Sway Test 3, No Wind Sway Velocity (m/s)</p> 
	<p>MATLAB Simulation of the Heavy Weight Narrow Motor Scenario</p>	<p>Reference Model and Plant Sway Velocity and Yaw Rate</p> 	

Sway Test	Motion Capture	Yaw Rate	Sway Rate
4		<p>Sway Test 4, No Wind Yaw Rate (Degrees/Second)</p> 	<p>Sway Test 4, No Wind Sway Velocity (m/s)</p> 
	<p>MATLAB Simulation of the Heavy Weight Wide Motor Scenario</p>	<p>Reference Model and Plant Sway Velocity and Yaw Rate</p> 	

**Table 25 Yaw Test Data**

Yaw Test	Motion Capture	X Position	Y Position
1			
2			

Yaw Test	Motion Capture	X Position	Y Position
3		<p data-bbox="743 302 1050 350">Yaw Test 3, No Disturbances X Position in One Full Rotation (m)</p> 	<p data-bbox="1398 302 1705 350">Yaw Test 3, No Disturbances Y Position in One Full Rotation (m)</p> 
4		<p data-bbox="743 833 1050 881">Yaw Test 4, Wind Disturbance X Position in One Full Rotation (m)</p> 	<p data-bbox="1398 833 1705 881">Yaw Test 4, Wind Disturbance Y Position in One Full Rotation (m)</p> 

## F. Test Results

### *Sway Testing*

During sway testing, the controller adapted quickly to the unknown parameters while filtering the adaption signal from the control signal. Comparison of all four no wind sway tests show that the two tests with the greatest yaw errors are Sway Test 1 and Sway Test 4. The 2-norm errors for Sway Test 1 and Sway Test 4 were  $8.1^\circ/\text{second}$  and  $10^\circ/\text{second}$  while Sway Test 3 and Sway Test 4 have 2-norm errors of  $6.2^\circ/\text{second}$  and  $7.1^\circ/\text{second}$  respectively. Nonetheless, Figure 20 shows that the controller maintained an average yaw rate of zero over the length of the test.

The box plot of the same data in Figure 20 shows that, while the average yaw rate was approximately zero, the distribution is more heavily weighted in positive yaw. At the same time, the surge error (Figure 21) in the sway tests was also positive (forward displacement). Assuming surge and sway are not hydrodynamically coupled (e.g., the boat is symmetrical along the longitudinal axis), then any error in surge implies the force from the port and starboard motors are not matched. The root cause of a positive surge is likely one of two factors. Primarily, if the

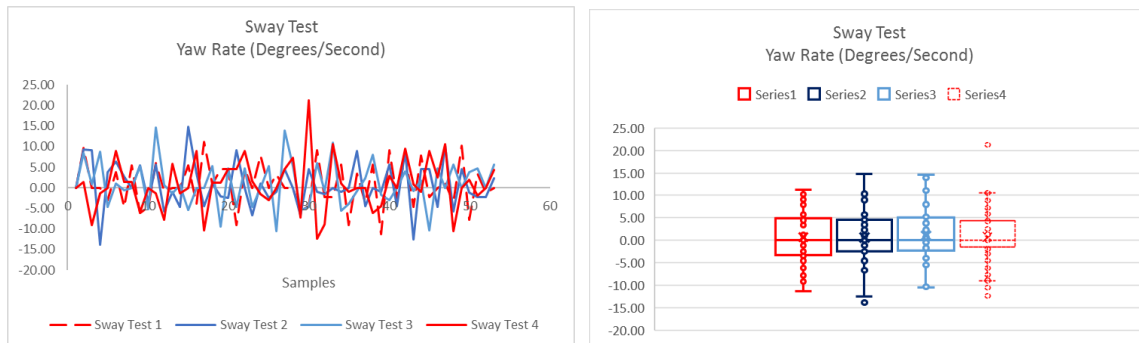


**Figure 20 Sway Test Yaw Rate Results, All Scenarios**

reverse propeller is not as efficient as the forward propeller, the generated thrust will be lower in

reverse than forward for the same speed setting. Secondly, the steering angle and/or speed control might not have been perfectly calibrated. Regardless of the root cause behind unmatched forward thrust, the imbalance created additional clockwise torque. Consequently, the final value for  $\psi$  in all tests was positive after 0.9 meter translations (three beam widths) which proves the controller was adapting as designed but not quite fast enough to meet specifications.

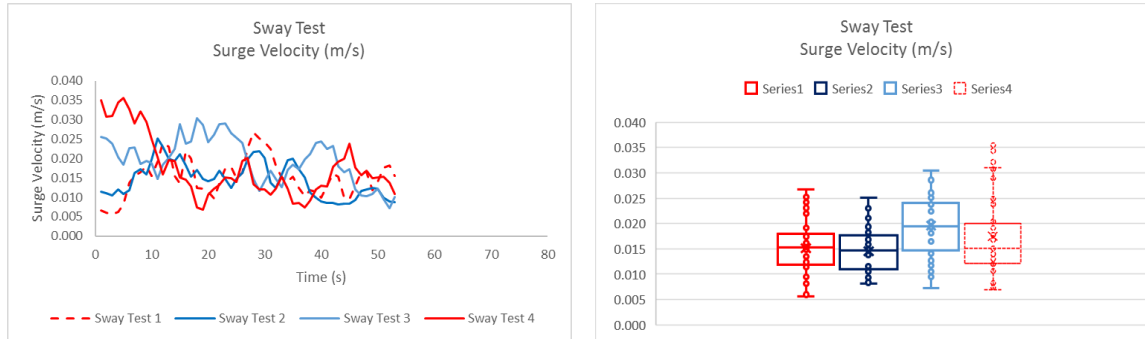


**Figure 21 Sway Test Surge Velocity Results, All Scenarios**

### *Yaw Testing*

During yaw testing, the controller adapted quickly to the unknown parameters and disturbances while filtering the adaption signal from the control signal within one full rotation. The best performing test, Yaw Test 3, completed a full rotation while moving only 0.02 m from the starting point which is 2% of the test boat length. The worst performing test, Yaw Test 4, moved 0.14m which is 12% of the test boat length as shown in Figure 22.

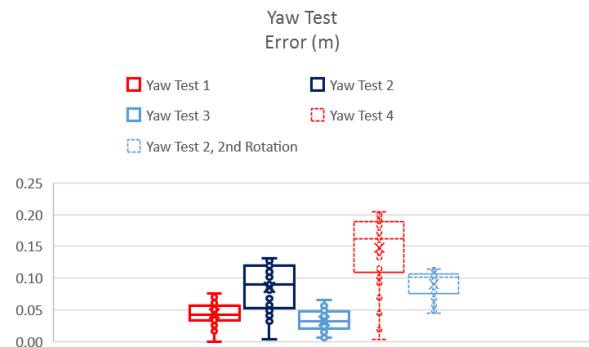


**Figure 22 Yaw Test Position Error Results**

The motion capture shows that within one-half of a rotation, the controller adapted not only to the load but also to the wind disturbance. In the face of the wind disturbance, the test boat made a second rotation in Yaw Test 2 in which the second rotation closely followed the second half of the first rotation all the way around (motion capture in red). Before the yaw test, data was collected to measure the strength of the wind. The data showed that, when the boat was dead in the water, the wind disturbance pushed the boat at about 0.09 m/s. Two full rotations required almost 90 seconds; therefore, in that time the wind would have pushed the boat 0.8 m or more if the controller did not adapt to the disturbance. Instead, in the second rotation, the 2-norm was less than half the error of the first rotation and even approached the error level of the disturbance-free Yaw Test 3 (one rotation). This means that the controller, as designed, was adapting to unknown parameters and disturbances.

#### G. Test Result Synthesis and Controller Refinements

The simulation and test data indicate that four design decisions enabled the L1AC controller's success. First, the controller needed a process for adapting to an unknown neutral position for yaw control. Second, the boundaries for the unknown plant parameters must be set properly. L1AC implementation required knowledge of the range of allowable boat configurations. The controller specifications included the minimum and maximum:

- Distance from the engine to the center of lateral resistance
- Reverse propeller efficiency
- Wind forces

Third, in sway maneuvering the controller performance was sensitive to the moment generated by the propulsion system. If the nominal power is set too low, the moment arm was too weak to



provide effective control. If the nominal was too high, then the moment arm over-powered the

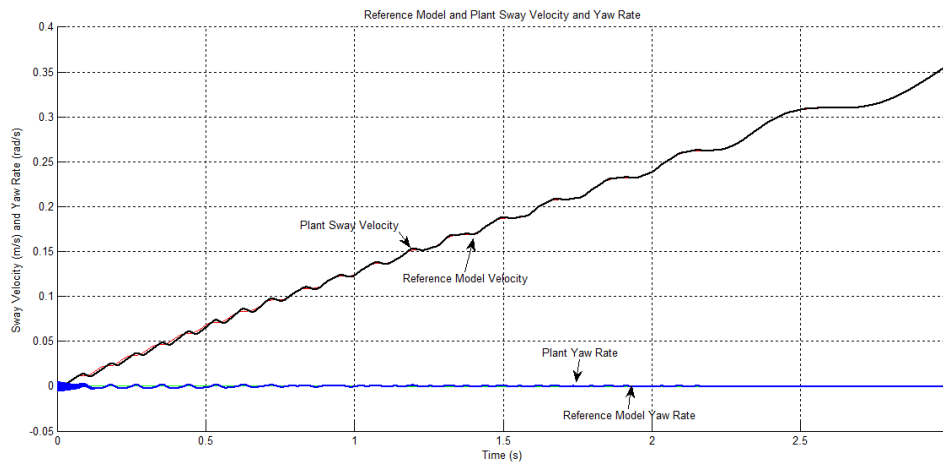


**Figure 23 Heavy Weight Wide Motors Fixed Nominal Power**

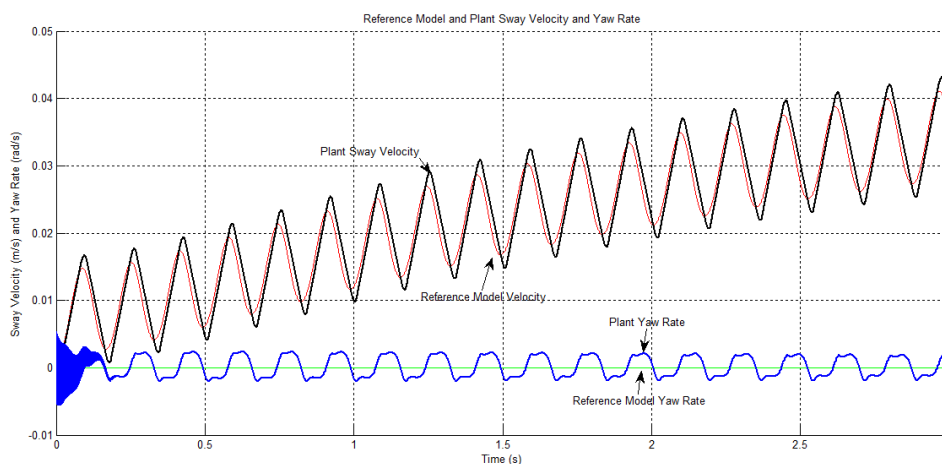


**Figure 24 Heavy Weight Wide Motors Modulated Nominal Power**

boat creating oscillations. As an improvement, the controller could modulate the base power as function of the sine of the rudder angle. MATLAB simulations in Figures 23 and 24 below quantify the potential improvement on the boat's controllability. Figure 23 predicts a yaw rate oscillation centered around zero yaw rate but with a positive bias which is the same as the test result. Figure 24 predicts the yaw rate will be damped considerably when the power is modulated. Fourth, the sway test performance errors reflected the surge errors. Table 26 shows

the rank order of decreasing surge and yaw rate errors for each test scenario. This could indicate that the yaw control was more sensitive to surge than previously expected.

**Table 26 Sway Test Rank Order by Maximum Surge and Yaw Rate Error**

<b>Rank by</b>	<b>Sway Test 1</b>	<b>Sway Test 2</b>	<b>Sway Test 3</b>	<b>Sway Test 4</b>
Maximum surge error	2 <sup>nd</sup>	1 <sup>st</sup>	3 <sup>rd</sup>	4 <sup>th</sup>
Maximum yaw rate error	2 <sup>nd</sup>	1 <sup>st</sup>	3 <sup>rd</sup>	4 <sup>th</sup>

## VI. CONCLUSIONS AND OPPORTUNITIES FOR FURTHER RESEARCH

### A. Conclusions

Research to create an L1 Adaptive Control methodology for commissioning a joystick steering system without the need for unique boat calibration was completed. By following a model based, systems engineering approach a working methodology was created for the target boat applications. The target applications cover a wide range of hull shapes and sizes; however, the target propulsion systems did not make use of bow or stern thrusters. During the physical and mathematical modeling of the target application, the research identified three main obstacles which the adaptive controller had to overcome:

- Lack of a dedicated yaw rate control actuator
- Unknown center of lateral resistance
- Lack of persistent excitation

This insight led to the selection of the L1 Adaptive Control architecture which provided the following key features:

- Guaranteed fast adaption
- Decoupled adaption and robustness
- Guaranteed transient performance

The above features made it possible for the adaption processes to overcome the three main obstacles mentioned above during slow speed maneuvering in calm seas with or without wind in a way that did not command unnecessary oscillations in the actuator control signals. Ultimately,

the methodology proved successful in MATLAB simulation and was further verified in controlled, scale boat testing of two critical maneuvers: stationary rotation and pure sway translation. The stationary rotation specification required the controller adapt fast enough to make one full rotation without changing position by one boat length or 1.2 meters. The average error for all scenarios (with and without wind disturbances) was 0.08 meters. The pure sway translation specification required the controller to adapt fast enough to translate three beam-widths without rotating ten degrees. The average error for all scenarios was 11.9 degrees. Though opportunities were identified to improve the test boat's performance, L1 Adaptive Control methodology was created from which a full control strategy could be built to eliminate the need for individual boat calibrations.

## B. Contributions

The research created primary and secondary contributions to engineering joystick steering for recreational boats. The primary contribution was the application of L1 Adaptive Control to a scaled version of the target application in stationary rotation and sway translation. In industry today, the target applications use unique calibrations to control the propulsion system while relying on the captain to manually counter any calibration errors or disturbance forces. The secondary contributions include the development of methodologies to overcome the obstacle of unknown neutral position for yaw control as well as the methodology for creating a linear torque input as a function of steering angle. The above novel solutions to the joystick steering control strategy were critical to completing the research.

### C. Implications for Application

While the research met the success criteria established at the onset, the methodology developed requires further research before it could be ready for commercialization. Focus areas for extended research could include improved methodologies for detailed controller design, full motion control, strategies for three and four engine configurations, application to new boat types (i.e., pontoon boats), and lastly, a methodology for testing the limits of robustness in the presence of wind and waves. Once complete, the methodology could be understood enough for full scale development and test.

First, the design process itself could be refined. Research areas would include a process for optimizing the filter design, defining the reference boat, optimizing the range of allowable parameters for a given reference system, and defining the base power level. For the research, the filter was designed through trial and error; however, a more sophisticated process could be developed. Also, there is a tradeoff between the reference boat and robustness. If the reference boat performance is too aggressive, robustness could become limited. Likewise, there is a tradeoff between performance and robustness when defining the allowable range of values in the adaptive parameters. For example, during the control design the minimum and maximum values of the plant parameters must be programmed into the Adaptive Law. The narrower the range, the faster the adaptation. On the other hand, the narrower the range, the narrower the target application for any specific controller design. The above processes should be refined before starting full scale development.

Likewise, a full control strategy would need to be created. The research focused solely on stationary rotation and sway translation. For simplicity, the controllers for each maneuver were created separately and only one code set was engaged at a time. For commercialization, the controller would need to respond to changing inputs including commands to combine surge, sway, and rotation maneuvers.

Commercialization would also require additional development for specific engine configurations and possibly new boat types. The research was limited to boat configurations with two motors. Full scale applications can have three or four. Thus, the control allocation could have even more flexibility. Just as the methodology would need to be expanded to include more than two engines, it could be expanded to include more target boat types than today. The adaptability of the test boat implies that smaller, lighter boat categories such as pontoons boats might also be candidates for joystick control. In the smaller boat segments, it is much more likely that the center of lateral resistance will vary from trip to trip as the crew and gear load outs have a greater effect on the overall center of gravity of the boat. This feature of small boats would preclude joystick steering without adaptive control. Additionally, it is interesting to note that pontoon hull forms are significantly different than the deep V focus of this research. Therefore, before commercialization, research would need to investigate all available engine configurations as well as potential new target applications.

Lastly, reflecting on the test boat's adaptability in the face of the wind disturbance, the research also implies there could be an opportunity to research how to characterize the limits of the controller's disturbance rejection. That is, further research could be conducted to find the

controller's limitations in compensating for large waves, strong winds, and/or fast currents. The fast adaption of the LIAC methodology might make joystick control even more intuitive for maneuvering in harsh environments or as a DP controller.

## VII. BIBLIOGRAPHY AND REFERENCES

- Anderson, Brian. (2005) "Failures of Adaptive Control Theory", *Communications in Information and Systems*, Vol 5, No.1, pp 1-20, 2005.
- Annaswamy A. a. (1989). *Stable Adaptive Systems*. Mineola, New York: Dover Publications Inc.
- Barrass, C.B. and Derrett, D.R. (2006) *Ship Stability for Masters and Mates*. 6th Edition. Oxford, UK. [Section 8.13] Butterworth-Heinemann.
- Bertram, V. (2000) *Practical Ship Hydrodynamics*. Oxford, UK. [Sections 8.16, 8.17] Butterworth-Heinemann.
- Craig, Kevin. (2012) "Modeling Engineering Systems." *Fluid Power Systems and Control*. Marquette University. Milwaukee. Lecture.
- Fossen, T. (2011). *Handbook of Marine Craft Hydrodynamics and Motion Control*. Sussex, United Kingdom: John Wiley & Sons Ltd.
- "Maneuvering Models." Fossen, Thor. NTNU. Web. 09 Mar. 07.
- "Lecture -2 Components of Resistance – II." Misra, S. C. IIT Kharagpur. Web. 14 May 08.
- "The 22 - An Affordable Custom Center Console." Harrisonboatworks. Web. ND.
- Hovakimyan, Naira (2010). *L1 Adaptive Control Theory Guaranteed Robustness with Fast Adaptation*. Philadelphia, PA: Society for Industrial and Applied Mathematics.
- P. Ioannou, K. S. Narendra, A. M. Annaswamy, S. Jafari, L. Rudd, R. Ortega, and J. Boskovic (2012). *L1-Adaptive Control: Stability, Robustness, And Misperceptions*. IEEE Transactions on Automatic Control.
- Jouffroy, J. a. (2012). Modeling and Nonlinear Heading Control of Sailing Yachts. *IEEE Journal of Oceanic Engineering*, 1-13.



"Joystick Docking." Joystick Docking Volvo Penta. Web. 15 Feb. 16.

Kanellakopoulos, J. a. (1995). *Nonlinear and Adaptive Control Design*. New York, New York: John Wiley & Sons Ltd.

K. K., Appuu Kuttan. (2007). *Introduction to Mechatronics*. Oxford University Press.

Lamb, Thomas. (2003 - 2004). *Ship Design and Construction, Volumes 1-2*. Society of Naval Architects and Marine Engineers (SNAME).

Larsson, Lars Raven, Hoyte C.. (2010). *Principles of Naval Architecture Series - Ship Resistance and Flow*. Society of Naval Architects and Marine Engineers (SNAME).

Lemancik, Michael. Personal Interview. 25 May 2009.

Lewis, Edward V.. (1988). *Principles of Naval Architecture (Second Revision), Volume II - Resistance, Propulsion and Vibration*. Society of Naval Architects and Marine Engineers (SNAME).

Liao, Y. a. (2010). *Combined Speed and Yaw Control of Underactuated Unmanned Surface Vehicles*. *2nd International Asia Conference on Informatics in Control, Automation, and Robotics* (pp. 157-161). Harbin, China: National Key Laboratory of Science and Technology on Autonomous Underwater Vehicle.

Mercury Marine. *Joystick Piloting for Outboards*. Fond Du Lac: Mercury Marine, 2014. Print.

Molland, Anthony F.. (2008). *Maritime Engineering Reference Book - A Guide to Ship Design, Construction and Operation*. Elsevier.

"Motor Control with Arduino: A Case Study in Data-Driven Modeling and Control Design." Mathworks. Web. 2013.

Rawson, K.J. Tupper, E.C.. (2001). *Basic Ship Theory (5th Edition)*. Elsevier.

Svendsen, C. H. (2012). *L1 Adaptive Manoeuvring Control of Unmanned High-speed Water Craft*. In Proceedings of the 9th IFAC Conference on Manoeuvring and Control of Marine Crafts. (pp. 144-151).

Tupper, Eric C.. (2004). Introduction to Naval Architecture (4th Edition). Elsevier.

Van Kleeck, John (DATE). *Formation Control for Autonomous Marine Vehicles*. University of Alberta.

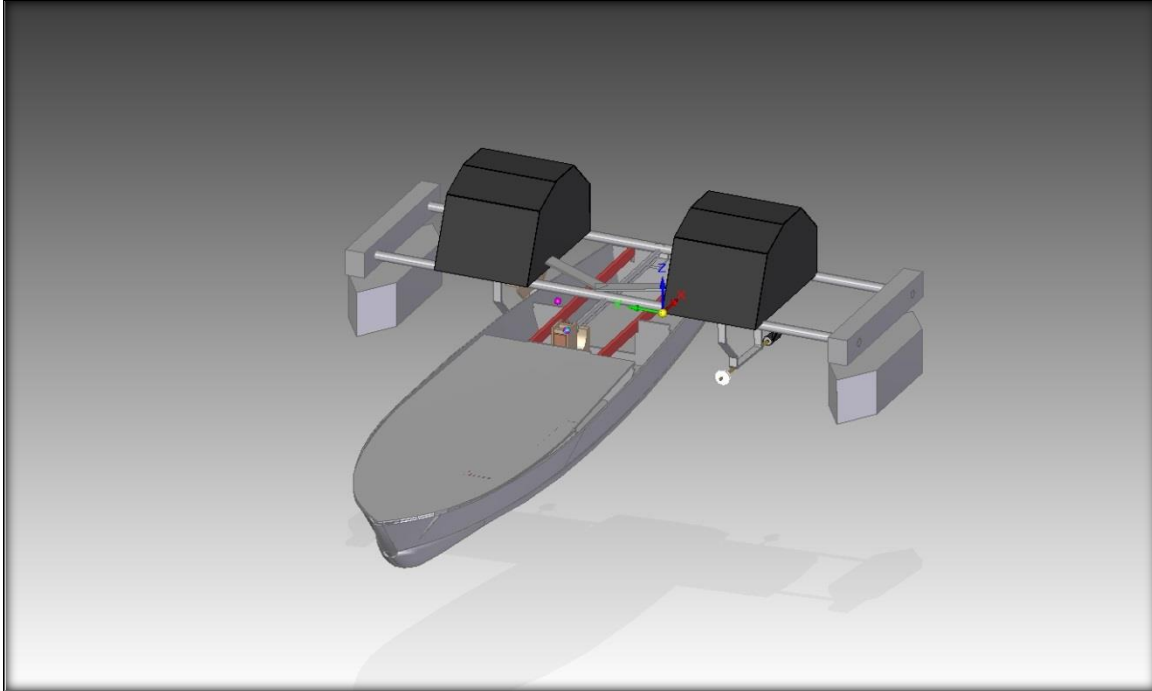
Verma, R. K. (2004). *Dynamic Positioning of Ship Using Direct Model Reference Adaptive Control*. Kingsville, TX: Texas A&M University.

"Video Physics for iPhone, iPad, and iPod Touch." Vernier Software and Technology. 2016. Web.

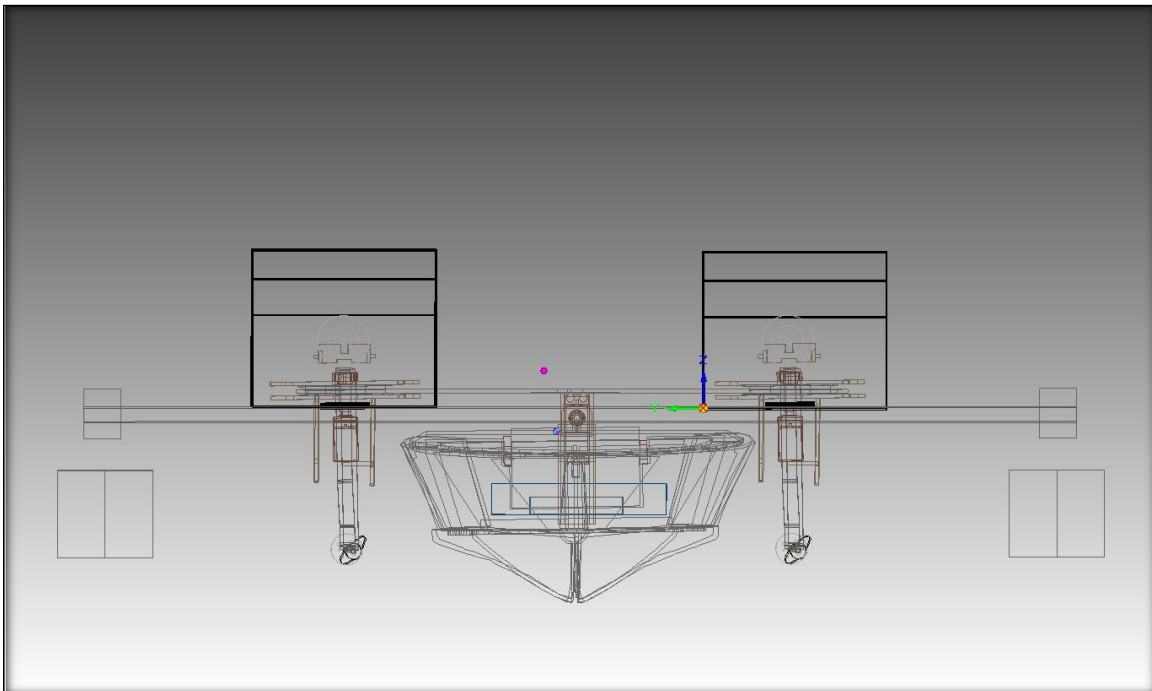
## APPENDIX A Test Boat and Joystick Target Applications

Figures 25-27 are screenshots taken from the test boat's CAD assembly model.

**Figure 25 Test Boat CAD Assembly**



**Figure 26 Test Boat CAD Assembly Wire Diagram**



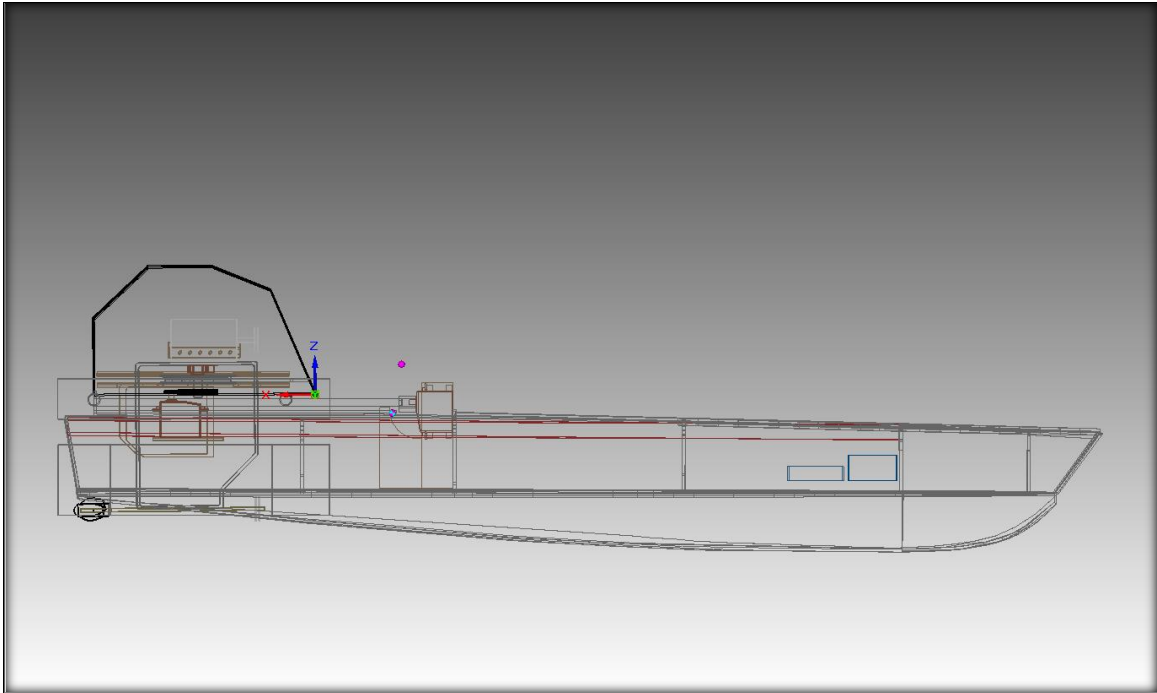


Figure 28 includes two pictures of a custom center console boat under construction. Note the similarities in hull form and construction techniques between Figures 26 and 27 below. Figure 29 is a picture of the test boat hull.

**Figure 27 Full Scale Center Console Plywood Fishing Boat Construction**



**Figure 28 Full Size Custom Center Console Boat Under Construction**



**Figure 29 Test Boat Hull**

## APPENDIX B Physical System Details

Table 27 Physical System

Test Boat Parameter	Description	Initial Estimate	Units	Source
<b>M</b>	Total mass	4.6	Kg	SolidEdge
<b>I<sub>xx</sub></b>	Inertia	0.3	Kg/m <sup>2</sup>	SolidEdge
<b>I<sub>zz</sub></b>	Inertia	2.2	Kg/m <sup>2</sup>	SolidEdge
<b>3I<sub>xz</sub></b>	Inertia	0.4	Kg/m <sup>2</sup>	SolidEdge
<b>G</b>	Center of Gravity	X: -0.7 Y: 0.0 Z: -0.07	m	SolidEdge
<b>L</b>	Length at the waterline	1.2	m	SolidEdge/Calculation
<b>B</b>	Beam	0.3	m	SolidEdge
<b>C<sub>B</sub></b>	Block Coefficient	0.86	NA	(Lamb, 11-10)
<b>T</b>	Depth below waterline	0.06	m	SolidEdge/Calculation
From Lewis (1988):				
$-\frac{Y'_v}{\pi \left(\frac{T}{L}\right)^2}$	Hydrodynamic derivative	1.37	NA	Semi-empirical Heuristic
$-\frac{Y'_r}{\pi \left(\frac{T}{L}\right)^2}$	Hydrodynamic derivative	0.09	NA	Semi-empirical Heuristic
$-\frac{N'_v}{\pi \left(\frac{T}{L}\right)^2}$	Hydrodynamic derivative	0.07	NA	Semi-empirical Heuristic
$-\frac{N'_r}{\pi \left(\frac{T}{L}\right)^2}$	Hydrodynamic derivative	-0.84	NA	Semi-empirical Heuristic
$-\frac{Y'_v}{\pi \left(\frac{T}{L}\right)^2}$	Hydrodynamic derivative	2.72	NA	Semi-empirical Heuristic
$-\frac{Y'_r}{\pi \left(\frac{T}{L}\right)^2}$	Hydrodynamic derivative	-0.35	NA	Semi-empirical Heuristic
$-\frac{N'_v}{\pi \left(\frac{T}{L}\right)^2}$	Hydrodynamic derivative	0.62	NA	Semi-empirical Heuristic
$-\frac{N'_r}{\pi \left(\frac{T}{L}\right)^2}$	Hydrodynamic derivative	0.31	NA	Semi-empirical Heuristic

## APPENDIX C Materials

**Table 28 Materials List**

<b>Materials</b>	<b>Description</b>
CAD Software	SolidEdge
Simulation Software	MATLAB
Test Boat Hull	1/24 scale scratch-built wooden boat with ballast compartments and adjustable motor placement
Propulsion System	Belt driven propeller powered by DC motors
Steering System	Servo powered turret mechanism
Control Computer	Arduino Uno
Sensors	Bosch BNO055
Measurement Device and Software	iPhone 6 and Video Physics Logger Pro
Test Tank	1.5m x 3.0m x 0.1m indoor water tank
Wind Generator	AC powered household fan

## APPENDIX D MATLAB Projection Operator

```

unction [projection]=projection_operator(y,estimate,theta,epsilon)
% Thesis Research
% This is the projection operator used for L1AC Adaptive Laws
% John Bayless, September 2016
% Reference:
% Hovakimyan, Naira (2010). L1 Adaptive Control Theory Guaranteed
% Robustness with Fast Adaptation. Philadelphia, PA:
% Society for Industrial and Applied Mathematics
%
f = (estimate'*estimate-
max(theta).*max(theta))./(epsilon*max(theta).*max(theta));
df = 2*estimate/(epsilon*max(theta)*max(theta));
dfy = df'*y;
%
dfsquared = df.*df;
sumofdfelements = sum(sum(dfsquared));
sqrtdfsquared = (sumofdfelements)^0.5;
if sqrtdfsquared > 0
    norm = df./sqrtdfsquared;
else
    norm = df.*0;
end
normdoty = sum(norm.*y);
normdotyxnorm = normdoty*norm;
ndotyxnormxf = normdotyxnorm*f;
yminusndotyxnormxf = y - ndotyxnormxf;

if f < 0
    projection = y;
else
    if dfy <- 0
        projection = y;
    else
        projection = yminusndotyxnormxf;
    end
end
end
end

```

## APPENDIX E Test Plan and Test Procedure

To run each scenario, the test boat was placed at rest in an indoor test tank until the controller engaged. The test tank was approximately 1.5m x 3.0m x 0.1m in dimension. The two maneuvers included:

1. Sway translation (sway test)
2. Stationary rotation (yaw test)

The four scenarios included:

1. Narrow engine to engine center distance, aft center of gravity
2. Narrow engine to engine center distance, forward center of gravity
3. Wide engine to engine center distance, after center of gravity
4. Wide engine to engine center distance, forward center of gravity

The digital video was captured by an iPhone6 placed in a stationary boom approximately 1.7m above the water. The video was then processed by the software, *Video Physics*. The software tracked a blue LED light positioned amidships. Based on the object tracking, the software created the estimates for position and velocity over time in the inertial reference frame.

The detailed test procedure is outlined in Table 29 below:



**Table 29 Test Procedure**

<b>Test Maneuver</b>	<b>Test Procedure</b>
Sway Test	<ol style="list-style-type: none"> <li>1. Turn off the controller</li> <li>2. Set the motor to motor distance</li> <li>3. Add ballast as required</li> <li>4. Turn on the video recorder</li> <li>5. Place the boat at the North end of the test tank, facing East</li> <li>6. Turn on the controller</li> <li>7. Release the boat such that the boat is at rest</li> <li>8. When the boat reaches the South end of the test tank, turn off the controller</li> <li>9. Upload the video to the motion tracking software</li> <li>10. Align the tracking tool with the blue LED control indication light</li> <li>11. Set the motion tracking scale based on the distance between deck features</li> <li>12. Export test data for analysis</li> </ol>
Yaw Test	<ol style="list-style-type: none"> <li>1. Turn off the controller</li> <li>2. Set the motor to motor distance</li> <li>3. Add ballast as required</li> <li>4. Turn on the video recorder</li> <li>5. Place the boat in the middle of the test tank facing East</li> <li>6. Turn on the controller</li> <li>7. Release the boat such that the boat is at rest</li> <li>8. Let the boat rotate for at least 360° and then turn off the controller</li> <li>9. Upload the video to the motion tracking software</li> <li>10. Align the tracking tool with the blue LED control indication light</li> <li>11. Set the motion tracking scale based on the distance between deck features</li> <li>12. Export test data for analysis</li> </ol>

## APPENDIX F Yaw Maneuver Error Calculations

The ideal position was estimated based on the average yaw rate for each rotation as follows:

$$\psi_n^* = \frac{t_n}{T} 2\pi$$

Where

$\psi_n^*$  = *nominal yaw angle at data point n*

$t_n$  = *elapsed time at data point n*

$T$  = *total actual time to complete a single rotation*

And

$$x_n^* = 0.183 * \cos(-\psi_n^*)$$

$$y_n^* = 0.183 * \sin(-\psi_n^*)$$

$$x_{n \text{ error}} = x_n^* - x_n$$

$$y_{n \text{ error}} = y_n^* - y_n$$

$$error_n = \sqrt{(x_n^* - x_n)^2 + (y_n^* - y_n)^2}$$

Where

0.183 = *distance from the origin to the tracking light*

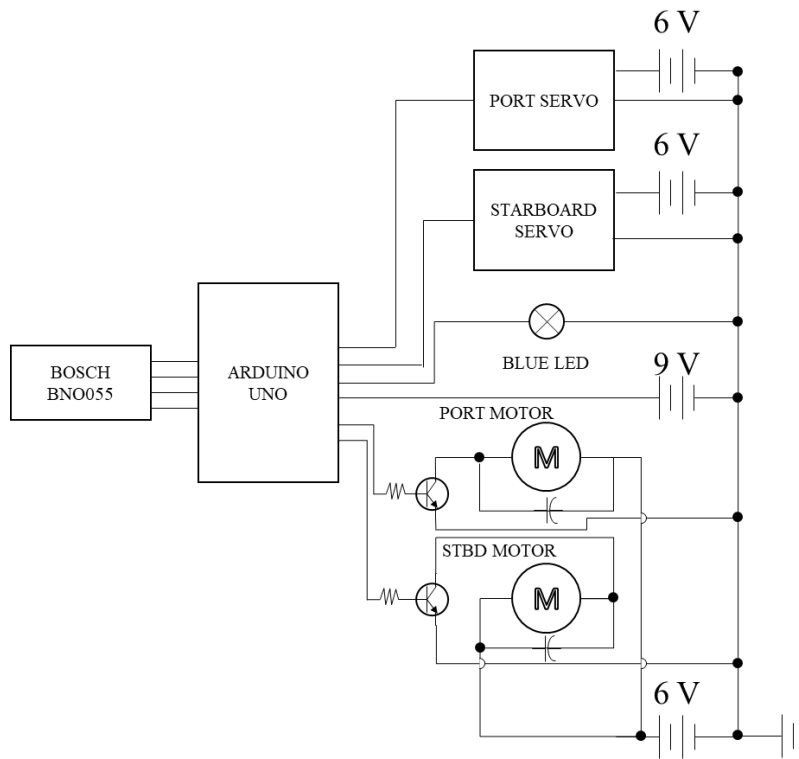
$x_n^*$  = *ideal X position at data point n*

$y_n^*$  = *ideal Y position at data point n*

$x_n$  = *actual X position at data point n*

$y_n$  = *actual Y position at data point n*

## APPENDIX G Wiring Diagram



## APPENDIX H Arduino Control Code for Sway Maneuvers

```
/*  
    John Bayless  
    M.S. Mechanical Engineering  
    L1AC Joystick Control  
    November, 2016  
*/  
  
// declare actuator variables  
const int portservoMin = 86;  
const int portservoMax = 128;  
const int starbservoMin = 50;  
const int starbservoMax = 92;  
double yawcontrol;  
double rudder;  
double portrudder;  
double starbrudder;  
const int portbmotorMin = 50;  
const int portmotorMax = 255;  
const int starbmotorMin = 50;  
const int starbmotorMax = 255;  
const int nominalpower = 150;  
double starbpower;  
  
// declare model variables  
double surge_a;  
double sway_a;
```

```
double yaw_a;
double heading_a;
double headinghold;
double surge[3] = {0, 0, 0};
double sway[3] = {0, 0, 0};
double yaw[3] = {0, 0, 0};
double heading[3] = {0, 0, 0};
double m_surge[3] = {0, 0, 0};
double m_sway[3] = {0, 0, 0};
double m_yaw[3] = {0, 0, 0};
double surge_e;
double sway_e;
double yaw_e;
double theta_1[2] = {0, 0};
double theta_1_proj;
double theta_1d;
double theta_1_min = 0.9;
double theta_1_max = 1.1;
double theta_23[2] = {0.5, 0.5};
double theta_23_proj;
double theta_23d;
double theta_23_min = 0.5;
double theta_23_max = 2;
double omega_1[2] = {0, 0};
double omega_1_proj;
double omega_1d;
double omega_1_min = 1;
double omega_1_max = 1.8;
```

```
double omega_23[2] = {1, 1};
double omega_23_proj;
double omega_23d;
double omega_23_min = 1;
double omega_23_max = 1.5;
double sigma_1[2] = {0, 0};
double sigma_1d;
double sigma_1_min = 0.01;
double sigma_1_max = 0.02;
double sigma_2[2] = {0.9, 0.9};
double sigma_2d;
double sigma_2_min = 0.01;
double sigma_2_max = 0.2;
double sigma_3[2] = {0.9, 0.9};
double sigma_3d;
double sigma_3_min = 0.01;
double sigma_3_max = 0.2;
double ETA_1;
double ETA_2;
double ETA_3;
double r_1 = 0;           // commanded velocities
double r_2 = 0.07;
double r_3 = 0;
double R_1[3];           // input to actuator filter
double R_2[3];
double R_3[3];
double kg_1 = 0.8;
double kg_2 = 0.7143;
```

```
    double kg_3 = 1;
double U_1[3] = {0, 0, 0};
    double U_2[3] = {0, 0, 0};
    double U_3[3] = {0, 0, 0};

// declare IMU variables
const int numReadings = 4;
double surgereadings[5];
double yawreadings[5];
double swayreadings[5];
double headingreadings[5];
int readIndex = 0;
double surgetotal = 0;
double swaytotal = 0;
double yawtotal = 0;
double headingtotal = 0;

// configure the servos
#include <Servo.h>
Servo portservo;
const int portservoPin = 9;
Servo starbservo;
const int starbservoPin = 10;

// configure the sensor
#include <Wire.h>
#include <Adafruit_Sensor.h>
#include <Adafruit_BNO055.h>
```

```
#include <utility/imumaths.h>
Adafruit_BNO055 bno = Adafruit_BNO055(55);

// configure the tracking LED
const int ledpin = 12;

// configure the motors
const int portmotorPin = 5;
const int starbmotorPin = 6;

// configure the timer
double timer;
double T_s = 0.08;

// configure set up

void setup() {

  Serial.begin(9600);
  Serial.println("Orientation Sensor Test"); Serial.println("");

  /* Initialise the sensor */
  if (!bno.begin(Adafruit_BNO055::OPERATION_MODE_COMPASS))
  //if(!bno.begin())
  {
    /* There was a problem detecting the BNO055 ... check your connections */
    Serial.print("Ooops, no BNO055 detected ... Check your wiring or I2C ADDR!");
```



```
    while(1);
}

delay(1000);

bno.setExtCrystalUse(true);

// For servo set-up
portservo.attach(portservoPin);
starbservo.attach(starbservoPin);
portservo.write(116); // reference angle = 86
starbservo.write(62); // reference angle = 92
delay(5000);

// For motor control
pinMode(portmotorPin, OUTPUT);
pinMode(starbmotorPin, OUTPUT);

// Turn on the tracking light
pinMode(ledpin, OUTPUT);
delay(2000);
digitalWrite(ledpin, HIGH);
//analogWrite(starbmotorPin, nominalpower);
//analogWrite(portmotorPin, nominalpower-35);

// capture the initial heading
while (readIndex <= numReadings) {
```

```

headingtotal = headingtotal - headingreadings[readIndex];

// read the input from the IMU, take the integral for velocity
sensors_event_t event;

// bno.getVector(&event);
imu::Vector<3> vector =
bno.getVector(Adafruit_BNO055::VECTOR_MAGNETOMETER);
headingreadings[readIndex] = atan2(vector.y(), vector.x());
if(headingreadings[readIndex] <0) headingreadings[readIndex] =
headingreadings[readIndex] + 2*PI;

// add the latest reading to the total
headingtotal = headingtotal + headingreadings[readIndex];

// advance to the next position in the array
readIndex = readIndex + 1;
delay(1);
}
readIndex = 0;

headinghold = headingtotal / numReadings;

Serial.print("heading hold: ");
Serial.print(headinghold);
Serial.println("");
}

```

```

// main program
void loop() {

    // record loop start time
    timer = millis();

    // collect a number of acceleration data points for smoothing
    while (readIndex <= numReadings) {
        surgetotal = surgetotal - surgereadings[readIndex];
        swaytotal = swaytotal - swayreadings[readIndex];
        yawtotal = yawtotal - yawreadings[readIndex];
        headingtotal = headingtotal - headingreadings[readIndex];

        // read the input from the IMU, take the integral for velocity
        sensors_event_t event;

        // bno.getVector(&event);
        imu::Vector<3> linearaccel =
bno.getVector(Adafruit_BNO055::VECTOR_LINEARACCEL);
        surgereadings[readIndex] = linearaccel.x();
        swayreadings[readIndex] = linearaccel.y();

        imu::Vector<3> angularaccel = bno.getVector(Adafruit_BNO055::VECTOR_GYROSCOPE);
        yawreadings[readIndex] = angularaccel.z(); //57*

        Serial.println("");
        Serial.print("yaw: ");
        Serial.print(yawreadings[readIndex]);

```

```
Serial.println("");

imu::Vector<3> vector = bno.getVector(Adafruit_BNO055::VECTOR_MAGNETOMETER);
headingreadings[readIndex] = atan2(vector.y(), vector.x());
if(headingreadings[readIndex] < 0) headingreadings[readIndex] = headingreadings[readIndex]
+ 2*PI;

// add the latest reading to the total
surgetotal = surgetotal + surgereadings[readIndex];
swaytotal = swaytotal + swayreadings[readIndex];
yawtotal = yawtotal + yawreadings[readIndex];
headingtotal = headingtotal + headingreadings[readIndex];

// advance to the next position in the array
readIndex = readIndex + 1;
delay(1);
}
readIndex = 0;

// calculate the average accelerations
surge_a = surgetotal / numReadings; // saves new x[n]

sway_a = swaytotal / numReadings;

yaw_a = yawtotal / numReadings;
```

```

heading_a = headingtotal / numReadings;

// integrate the accerlations to find velocities
surge[1] = surge[0];
surge[0] = surge_a;

sway[1] = sway[0];
sway[0] = sway_a;

yaw[1] = yaw[0];
yaw[0] = (headi
ng[0] - heading_a)/T_s;

heading[1] = heading[0];
heading[0] = heading_a;

// calculate the refernce model velocities
m_surge[2] = m_surge[1];
m_surge[1] = m_surge[0];
m_surge[0] = 0.9048 * m_surge[1] - 0.04758 * U_1[1] * omega_1[0] + sigma_1[0] +
theta_1[0] * surge[0];

m_sway[2] = m_sway[1];
m_sway[1] = m_sway[0];
m_sway[0] = 1.93 * m_sway[1] - 0.9324 * m_sway[2] + theta_23[0] * sway[0] + (0.04998 *
U_2[1] - 0.0466 * U_2[2] - 0.001221 * U_3[1] - 0.9324 * U_3[2]) * omega_23[0] + sigma_2[0];

m_yaw[2] = m_yaw[1];

```

```

m_yaw[1] = m_yaw[0];

m_yaw[0] = 1.93 * m_yaw[1] - 0.9324 * m_yaw[2] + theta_23[0] * yaw[0] + (0.04827 *
U_3[1] - 0.04827 * U_3[2] + 0.001221 * U_2[1] + 0.001193 * U_2[2]) * 0.2118 * omega_23[0]
+ sigma_3[0] - 0.3529;

// calculate the error
surge_e = m_surge[0] - surge[0];

sway_e = m_sway[0] - sway[0];

yaw_e = m_yaw[0] - yaw[0];

// calculate the projection
// theta
theta_1_proj = -1 * surge_e * surge[0];
theta_1d = 10000 * theta_1_proj;
theta_1[1] = theta_1[0];
theta_1[0] = theta_1[1] + T_s * theta_1d;
theta_1[0] = constrain(theta_1[0],theta_1_min, theta_1_max);

theta_23_proj = -1 * yaw[0] * (0.5 * sway_e - ( 5 / 7 * yaw_e) - sway[0] * ((99 / 70 *
sway_e) - 0.5 * yaw_e));
theta_23d = 10000 * theta_23_proj;
theta_23[1] = theta_23[0];
theta_23[0] = theta_23[1] + T_s * theta_23d;
theta_23[0] = constrain(theta_23[0],theta_23_min, theta_23_max);

// omega
omega_1_proj = surge_e * U_1[0];
omega_1d = 20000 * omega_1_proj;

```

```

omega_1[1] = omega_1[0];
omega_1[0] = omega_1[1] + T_s * omega_1d;
omega_1[0] = constrain(omega_1[0],omega_1_min, omega_1_max);
omega_23_proj = -1 * U_3[0] * (0.5 * sway_e - ( 5 / 7 * yaw_e) - U_2[0] * ((99 / 70 *
sway_e) - 0.5 * yaw_e));
omega_23d = 10000 * omega_23_proj;
omega_23[1] = omega_23[0];
omega_23[0] = omega_23[1] + T_s * omega_23d;
omega_23[0] = constrain(omega_23[0],omega_23_min, omega_23_max);

// sigma
sigma_1d = 10000 * surge_e;
sigma_1[1] = sigma_1[0];
sigma_1[0] = sigma_1[1] + T_s * sigma_1d;
sigma_1[0] = constrain(sigma_1[0],sigma_1_min, sigma_1_max);
sigma_2d = 10000 * sway_e;
sigma_2[1] = sigma_2[0];
sigma_2[0] = sigma_2[1] + T_s * sigma_2d;
sigma_2[0] = constrain(sigma_2[0],sigma_2_min, sigma_2_max);
sigma_3d = 10000 * yaw_e;
sigma_3[1] = sigma_3[0];
sigma_3[0] = sigma_3[1] + T_s * sigma_3d;
sigma_3[0] = constrain(sigma_3[0],sigma_3_min, sigma_3_max);

// calculate ETA
ETA_1 = omega_1[0] * U_1[0] + theta_1[0] * surge[0] + sigma_1[0];

```

$$\text{ETA}_2 = \omega_{23}[0] * U_2[0] + \theta_{23}[0] * \text{sway}[0] + \sigma_2[0];$$

$$\text{ETA}_3 = \omega_{23}[0] * U_3[0] + \theta_{23}[0] * \text{yaw}[0] + \sigma_3[0];$$

// calculate R

$$R_1[2] = R_1[1];$$

$$R_1[1] = R_1[0];$$

$$R_1[0] = r_1 * kg_1 - \text{ETA}_1;$$

$$R_2[2] = R_2[1];$$

$$R_2[1] = R_2[0];$$

$$R_2[0] = r_2 * kg_2 - \text{ETA}_2;$$

$$R_3[2] = R_3[1];$$

$$R_3[1] = R_3[0];$$

$$R_3[0] = r_3 * kg_3 - \text{ETA}_3;$$

// calculate U

$$U_1[0] = U_1[1];$$

$$U_1[1] = U_1[0];$$

$$U_1[0] = 1.062 * U_1[1] - 0.08208 * U_1[2] + 0.03164 * R_1[1] - 0.01425 * R_1[2]; //0.01425 to 0.02425$$

$$U_2[2] = U_2[1];$$

$$U_2[1] = U_2[0];$$

$$U_2[0] = 1.082 * U_2[1] - 0.08208 * U_2[2] + 0.03164 * R_2[1] - 0.01425 * R_2[2];$$

$$U_3[2] = U_3[1];$$

$$U_3[1] = U_3[0];$$



```
U_3[0] = 1.082 * U_3[1] - 0.08208 * U_3[2] + 0.03164 * R_3[1] - 0.01425 * R_3[2];// +
2*(heading_a - headinghold);//0.03164 to 0.04164
```

```
// actuate the servos
```

```
yawcontrol = 115 * U_3[0]; //115
```

```
rudder = 3.3952 * yawcontrol - 5.49;
```

```
portrudder = 86 + rudder;
```

```
portrudder = constrain(portrudder, portservoMin, portservoMax);
```

```
portservo.write(portrudder);
```

```
starbrudder = 92 - rudder;
```

```
starbrudder = constrain(starbrudder, starbservoMin, starbservoMax);
```

```
starbservo.write(starbrudder);
```

```
// actuate the motors
```

```
analogWrite(starbmotorPin, nominalpower); // changed to make port adjust
```

```
starbpower = constrain(nominalpower - 0.30 * nominalpower + 1.3 * U_1[0], starbmotorMin,
starbmotorMax);// -8 adjustment for efficiency
```

```
analogWrite(portmotorPin, starbpower);
```

```
// delay until next sample time
```

```
timer = millis() - timer;
```

```
timer = (T_s * 1000) - timer;
```

```
delay(timer);
```

```
}
```